14 days after inoculation. AZD1152 (100 mg/kg) or the control Tris buffer was administered to mice by intraperitoneal injection on 2 consecutive days per week for 2 weeks starting on day 14 after inoculation. In both cell lines at 4 weeks after initiation of treatment, mice were sacrificed to assess the antitumor effects of AZD1152. The survival end points were defined as ascites formation in the hepatoma-bearing mice [30]. Animal survival data were entered in the Kaplan–Meier Life Table format and presented as the cumulative survival plot. Statistical differences were analyzed by Mantel–Cox log-rank test. All *in vivo* procedures were approved by the Animal Care Committee of Tokyo Medical and Dental University (Permission No. 090235).

The pharmacobiological effects of AZD1152 treatment in the orthotopic liver tumors were assessed by immunohistochemical analysis of PhH3 and cCasp-3 expression in control tumors and in those harvested 3 and 5 days after initiation of AZD1152 treatment.

Results

Aurora B kinase expression and in vitro effects of AZD1152-HQPA in human hepatocellular carcinoma cells

Evaluation of Aurora B kinase protein in 12 human HCC cell lines revealed a variety of expression levels, as shown in Fig. 1A (Aurora B/tubulin expression ratio: JHH-1, 0.120; JHH-2, 0.039; JHH-4, 0.059; HuH-1, 0.078; HuH-6, 0.220; HuH-7, 0.243; HLE, 0.040; HLF, 0.032; PLC/PRF/5, 0.083; SK-Hep1, 0.107; Hep3B, 0.079; HepG2, 0.044). Expression of Aurora B kinase was approximately 7-fold higher in HuH-7 and HuH-6 cells than in JHH-2 and HLF cells. To evaluate the growth inhibitory effects of AZD1152-HQPA, cell proliferation assays were conducted in these HCC cell lines. AZD1152-HQPA showed potent antiproliferative activity in all HCC cell types with IC_{50} values (JHH-1, 17.4 ± 1.0 nM; JHH-2, 218.0 ± 10.8 nM; JHH-4, 155.6 ± 16.8 nM; HuH-1, 27.3 ± 5.0 nM; HuH-6, 3.7 ± 0.6 nM; HuH-7, 6.8 ± 0.3 nM; HLE, 45.9 ± 6.4 nM; HLF, 126.1 ± 12.2 nM; PLC/PRF/5, 76.9 ± 9.9 nM; SK-Hep1, 21.9 ± 1.2 nM; Hep3B, 7.6 ± 1.2 nM; HepG2, 14.7 ± 1.7 nM) (Fig. 1A). Fig. 1B demonstrates the relationship between Aurora B kinase expression and indexes of AZD1152-HQPA IC_{50} in the panel of cell lines tested (correlation coefficient: −0.72738; $R^2 = 0.529$; $p = 0.0073$).

Alterations in DNA ploidy in the human HCC cell lines were analyzed by flow cytometry (Fig. 1C). Accumulation of cells with >4N DNA content was observed in all of the cell lines following

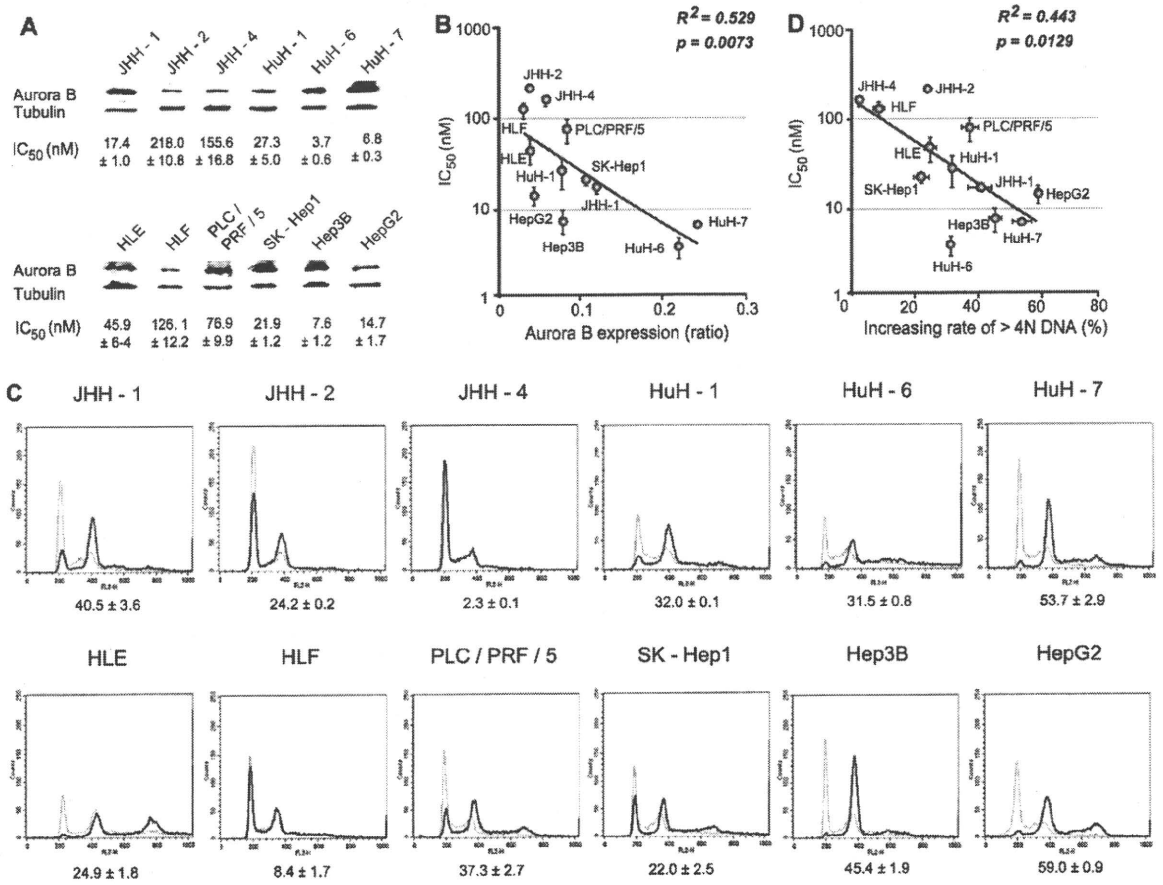

Fig. 1. Expression of Aurora B kinase and AZD1152-hydroxyquinazoline-pyrazol-anilide (AZD1152-HQPA) activity in human hepatocellular carcinoma (HCC) cell lines. (A) Western blot analysis of Aurora B kinase and the control alpha-tubulin. The concentration that induced half-maximal inhibitory concentration (IC_{50}) in 12 human HCC cell lines is indicated. (B) Relationship between the ratio of Aurora B kinase expression to control tubulin and the indexes of AZD1152 IC_{50} values in each human HCC cell line. Correlations were analyzed by Pearson two-tailed correlation. The level of statistical significance was $p < 0.05$. (C) Cellular DNA content was analyzed by flow cytometry in 12 human HCC cell lines after 24-h incubation with AZD1152-HQPA 100 nM (thick lines) or the control DMSO buffer (thin lines), and the increasing rate of >4N DNA (%) was indicated. (D) Relationship between the increasing rate of >4N cells and the indexes of AZD1152 IC_{50} values in each human HCC cell line. Correlations were analyzed by Pearson two-tailed correlation. The level of statistical significance was $p < 0.05$.

24-h incubation with AZD1152-HQPA 100 nM, with the exception of JHH-2 and HLF, which showed AZD1152 insensitivity with low expression levels of Aurora B kinase. As shown in Fig. 1D, the increasing rate of >4N DNA by AZD1152-HQPA (JHH-1, 40.5 ± 3.6%; JHH-2, 24.2 ± 0.2%; JHH-4, 2.3 ± 0.1%; HuH-1, 32.0 ± 0.1%; HuH-6, 31.5 ± 0.8%; HuH-7, 53.7 ± 2.9%; HLE, 24.9 ± 1.8%; HLF, 8.4 ± 1.7%; PLC/PRF/5, 37.3 ± 2.7%; SK-Hep1, 22.0 ± 2.5%; Hep3B, 45.4 ± 1.9%; HepG2, 59.0 ± 0.9%) was correlated with the indexes of IC_{50} values (correlation coefficient: −0.66534; $R^2 = 0.443$; $p = 0.0129$). The accumulation of polyploid cells is consistent with failed cytokinesis following inhibition of Aurora B kinase activity.

Previously, cellular apoptosis in response to the pan-Aurora kinase inhibitor VX680 was limited in cells expressing wild-type p53 but was enhanced in cells lacking p53 [31]. The p53 point mutations have been reported in four HCC cell lines (HuH-7 at codon 220 Tyr-to-Cys; HLF at codon 244 Gly-to-Ala; HLE and PLC/PRF/5 at codon 249 Arg-to-Ser), and null expression of p53 was reported due to the deletion in the Hep3B cell line, while SK-Hep1 and HepG2 have wild-type p53 [32–34]. There was no significant correlation between the efficacy of AZD1152-HQPA and the p53 status of each cell line in our experiments.

In vitro effects of AZD1152-HQPA on phosphorylation of histone H3 and cell death in human hepatocellular carcinoma cell lines

In the previous studies by Mortlock et al. [35], AZD1152-HQPA is a selective Aurora B kinase inhibitor with more than 1000- to 10,000-fold selectivity for Aurora A kinase and various tyrosine kinases including kinase insert domain receptor (KDR), the Abelson virus kinase (vABL), and epidermal growth factor receptor (EGFR). The inhibition of Aurora B kinase is determined by its specific cellular substrate histone H3 [36]. We investigated whether AZD1152-HQPA was able to inhibit PhH3 in the sensitive SK-Hep1 and Hep3B cells. As shown in Figs. 2 and 3a, AZD1152-HQPA 100 nM yielded a substantial reduction in the level of PhH3. This inhibition of histone H3 phosphorylation was shown to be dose dependent in SK-Hep1 and Hep3B cells treated with AZD1152-HQPA 1–100 nM (Fig. 3B). The cellular apoptosis was confirmed by analysis of Annexin-V binding (Fig. 3C). Cell death rates were measured and were also found be proportional to AZD1152-HQPA dose (Fig. 3D) [21]. These results indicate that inhibition of Aurora B kinase by AZD1152-HQPA can induce cell death in the SK-Hep1 and Hep3B cells *in vitro*. In contrast, the AZD1152-insensitive HLF cells with a low expression of Aurora B kinase (Fig. 1) showed no significant effects on PhH3 and apoptosis compared with SK-Hep1 and Hep3B cells (Figs. 2 and 3).

Fig. 2. Effects of AZD1152-hydroxyquinazoline-pyrazol-anilide (AZD1152-HQPA) on phosphorylation of histone H3 in human hepatocellular carcinoma (HCC) cell lines. Western blot analysis of phosphohistone H3 and the control alpha-tubulin in human HCC cell lines after 4-h incubation with AZD1152-HQPA 100 nM or the control DMSO buffer. Cell lines: SK-Hep1 (left), Hep3B (middle), and HLF (right).

In vivo effects of AZD1152 on subcutaneous xenografts of human hepatocellular carcinoma cells

The human HCC cell line SK-Hep1 (AZD1152 IC_{50}: 21.9 nM) is known to be aggressively tumorigenic *in vivo* [37]. To investigate *in vivo* antitumor activity, AZD1152 100 mg/kg per day was administered to nude mice bearing established SK-Hep1 subcutaneous xenografts on 2 consecutive days per week for 2 weeks ($n = 10$). Tumor volumes were measured every other day. As shown in Fig. 4A, significant regression of SK-Hep1 tumors was observed in the group of mice that received AZD1152 compared with control. The mean tumor volumes were substantially decreased by treatment with AZD1152 on day 14 following treatment, and tumor volumes in treated mice were 15.5% of those in control mice (Fig. 4B). None of the AZD1152-treated mice showed signs of wasting or other toxicity relative to control mice. AZD1152 was tolerated at the dose at which antitumor efficacy was observed.

In vivo effects of AZD1152 on orthotopic liver xenografts of human hepatocellular carcinoma cells

A novel orthotopic xenograft model of liver tumors with Matrigel was utilized to explore tumor growth inhibition in situ [25] (Fig. 5A). AZD1152 100 mg/kg was administered to mice bearing SK-Hep1 orthotopic xenografts on 2 consecutive days per week for 2 weeks ($n = 5$). Histological analysis of the liver tumors was conducted within 4 weeks after treatment. Growth of liver tumors was found to be suppressed in all of the mice that had been treated with AZD1152 (Fig. 5B). After drug administration, the mean liver tumor weight in those animals that had received AZD1152 was 10% of that in the control mice (Fig. 5C). Similar growth inhibition was observed in Hep3B orthotopic xenografts by administration of AZD1152 (Fig. 5B and C). In the orthotopic model, mouse survival was significantly enhanced by AZD1152 treatment in comparison with the control ($p < 0.005$; Fig. 5D). These results demonstrate that AZD1152 was able to significantly inhibit *in vivo* growth of a human HCC tumor in the liver microenvironment in mice. All of the host tissues examined, including liver, bone marrow, kidney, intestine, and lung, were histologically normal in all experiments.

Pharmacobiological effects of AZD1152 on orthotopic liver xenografts of human hepatocellular carcinoma cells

The liver xenograft model described above was subjected to histological analysis by immunostaining to investigate the pharmacobiological effects of AZD1152 in the hepatic microenvironment (Fig. 6). Three days after treatment with AZD1152, there was a substantial decrease in PhH3 (Fig. 6E and H) compared with the control (Fig. 6D and G), although after 5 days, PhH3 had recovered (Fig. 6F and I). Staining of tumor samples for apoptotic marker cCasp-3 showed gradually elevating levels following AZD1152 treatment (Fig. 6J–O). The hepatocytes from the host liver were histologically normal at all points following AZD1152 administration (Fig. 6A–C).

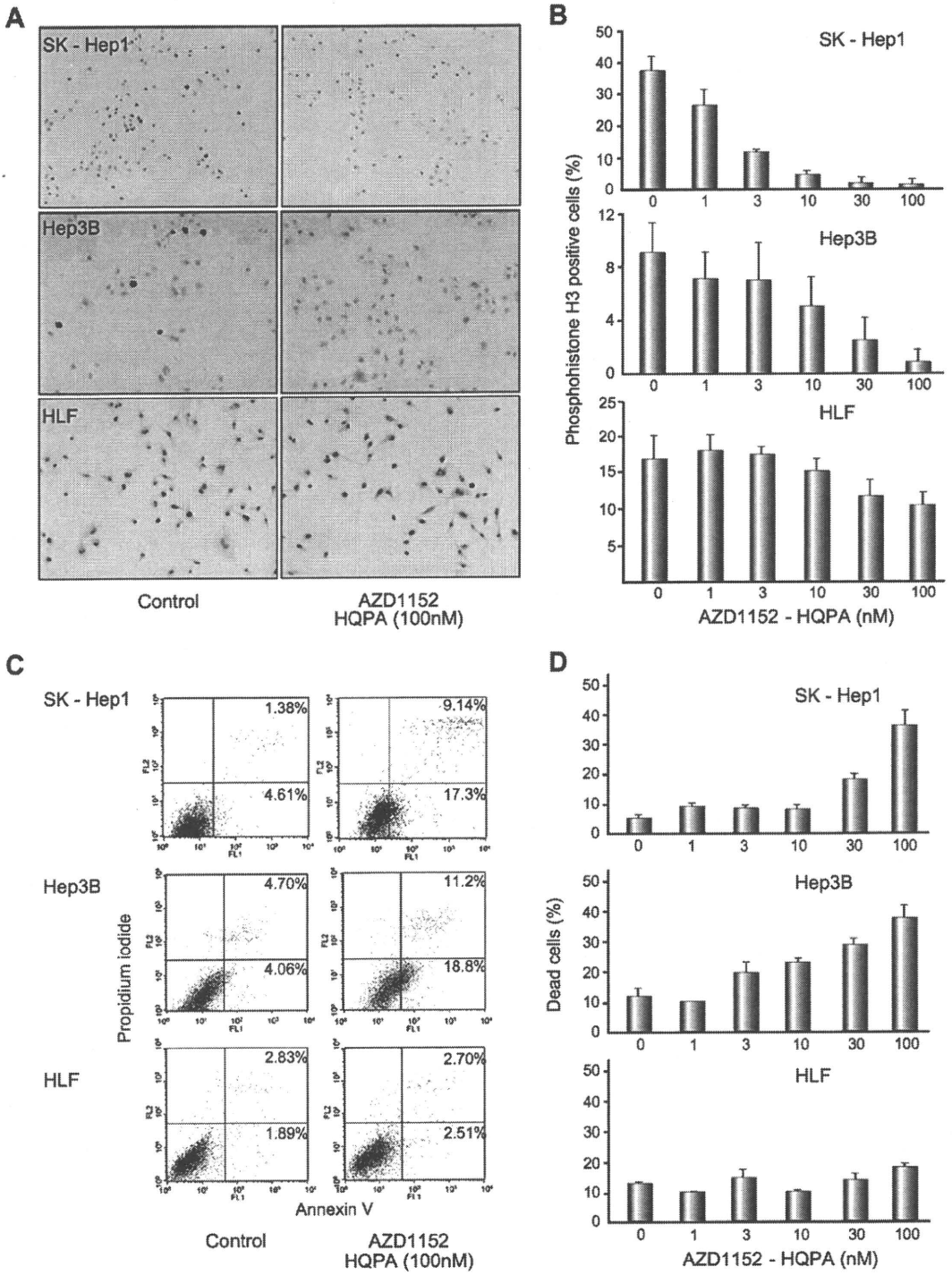

Fig. 3. Dose-dependent effects of AZD1152-hydroxyquinazoline-pyrazol-anilide (AZD1152-HQPA) on phosphorylation of histone H3 and cell death of human hepatocellular carcinoma (HCC) cell lines. (A) Immunocytochemistry of phosphohistone H3 (PhH3) in human HCC cells after 4-h incubation with AZD1152-HQPA 100 nM or the control DMSO buffer. Magnification ×200. Cell lines: SK-Hep1 (upper), Hep3B (middle), and HLF (lower). (B) Dose–response analysis showing percentage of PhH3-positive HCC cells analyzed by immunocytochemistry. Cell lines: SK-Hep1 (upper), Hep3B (middle), and HLF (lower). Columns, PhH3-positive cells (%); vertical bars, standard deviation. (C) AZD1152-HQPA induces apoptosis. SK-Hep1 (upper), Hep3B (middle), and HLF (lower) cells were treated with AZD1152-HQPA for 72 h, and apoptosis was assessed by flowcytometric analysis of cells labeled with Annexin V and propidium iodide. (D) Dose–response analysis showing percentage of nonviable cells in SK-Hep1, Hep3B, and HLF cell samples analyzed using a hemocytometer and trypan blue dye exclusion. Columns, dead cells (%); vertical bars, standard deviation.

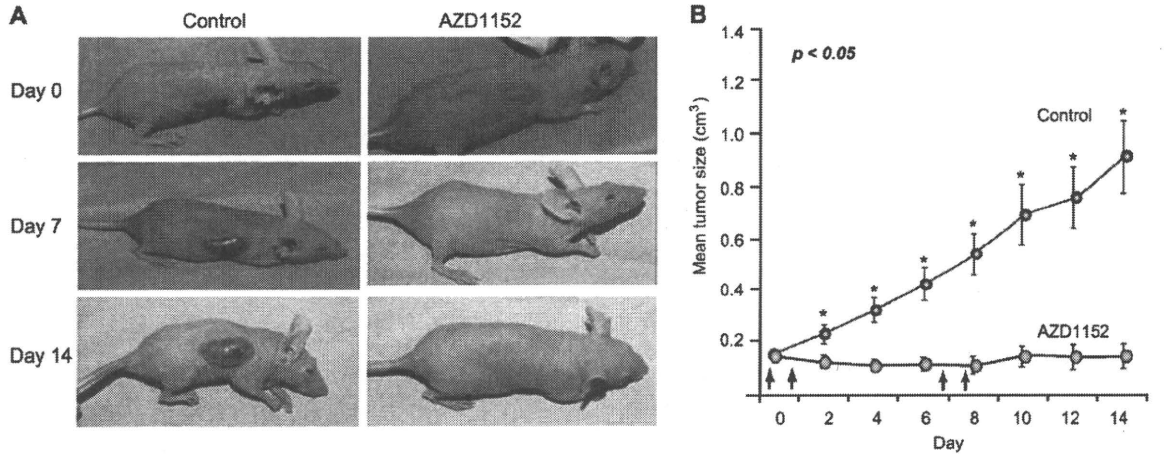

Fig. 4. *In vivo* effects of AZD1152 on human hepatocellular carcinoma (HCC) growth in subcutaneous xenograft models. Established subcutaneous xenografts of SK-Hep1 were treated with intraperitoneal AZD1152 100 mg/kg or the control Tris buffer on 2 consecutive days per week for 2 weeks. (A) Subcutaneous SK-Hep1 tumors in mice on days 0, 7, or 14 following treatment with AZD1152 (right) or the control (left). (B) Tumor volumes were measured and plotted every other day in AZD1152-treated or control mice ($n = 10$). Arrows, timing of administration; vertical bars; standard error. Statistical analysis was done by two-tailed Student t test (*$p < 0.05$).

Discussion

The Aurora family of serine–threonine kinases has recently emerged as a key mitotic regulator required for genome stability [38]. In mammals, the Aurora family consists of three members: Aurora A and B kinases and the less well-characterized Aurora C kinase. Aurora B kinase has been clearly shown to regulate kinetochore function, as it is required for correct chromosome alignment and segregation, spindle-checkpoint function, and cytokinesis. As Aurora kinases are frequently overexpressed in various tumors [39], they have received much attention as potential targets for novel anticancer therapeutics. Treatment with Aurora kinase inhibitors induces the accumulation of cells arrested in a pseudo-G1 state with >4N DNA content or the accumulation of cells with >4N DNA content, the latter population representing cells that exit mitosis and subsequently proceed through S phase in the absence of cell division [31]. Continued proliferation in the presence of aberrant mitosis and failed cytokinesis presumably gives rise to cells with higher DNA content due to an increase of the cell diameter, resulting in apoptosis [17,18,40,41]. The defective cytokinesis, as well as the inhibition of PhH3 by Aurora kinase inhibitors, suggests that the cellular effects of Aurora kinase inhibitors might be largely mediated by the disruption of Aurora B kinase function [18]. AZD1152 is a selective inhibitor of Aurora kinase with specificity for Aurora B kinase. AZD1152 has the potential to be efficacious in multiple tumor types and is currently undergoing phase 1 clinical evaluation as a treatment for a range of malignancies [20,21].

We have previously identified Aurora B kinase as the only independent predictor for the aggressive recurrence of human HCC [10]. In our present study, AZD1152-HQPA substantially reduced *in vitro* proliferation in a variety of human HCC cell lines. The extent of proliferation inhibition was correlated with Aurora B kinase expression levels (Fig. 1). As shown in Fig. 1C, significant DNA fragmentation in the form of a sub-G1 peak could not be detected after 24 h of treatment with AZD1152-HQPA, which is in line with data reported by Wilkinson et al. [20]. This inability to detect a sub-G1 population after AZD1152-HQPA treatment may result because inhibition of Aurora B kinase induces polyploidy before apoptosis, in which case DNA fragmentation will occur in the >4N population, making it difficult to detect a sub-G1 population.

Treatment with AZD1152-HQPA also led to inhibition of PhH3 as well as failure of tumor cell division, and ultimately induced death of human HCC cells (Figs. 2 and 3). *In vivo* administration of AZD1152 suppressed the growth of human HCC tumors in established subcutaneous xenografts (Fig. 4). Although subcutaneous xenograft models have the benefits of easy visualization and monitoring of tumor growth, the biological response to therapeutic agents in the natural microenvironment of the tumor should be analyzed using orthotopic xenograft models [30,42]. In this study, a novel model of intrahepatic inoculation with Matrigel was utilized to closely mimic HCC tumors in humans [24]. As shown in Fig. 5, AZD1152 inhibited *in vivo* growth of established liver tumors and increased survival in this model. Furthermore, pharmacobiological studies of AZD1152 confirmed *in vivo* suppression of PhH3 and induction of cellular apoptosis of human HCC (Fig. 6). AZD1152 was well tolerated at the dose required to elicit a potent and durable antitumor effect in mice. According to the previous report by Wilkinson et al. [20], mice were almost resistant to myelosuppression after AZD1152 treatment; the authors could not find any reductions in bone marrow nucleated cells at the end of the dosing period. In rats, there was a myelosuppressive effect of AZD1152 that was associated with a reduction in bone marrow nucleated cells to 34% of that seen in the controls at the end of the 48-h dosing period; however, the bone marrow nucleated cell content rapidly recovered such that it was 104.8% of control at the end of the study period. Although the phase 1 studies on the side effects of AZD1152 have not yet been reported in detail, humans might be more sensitive to the myelosuppressive effects compared to the experimental rodents. Further study should be required for clinical application to HCC patients, especially those with cirrhosis.

Clinical evidence exists indicating a significant relationship between Aurora B kinase expression and the aggressive progression of HCC [10], and our preclinical studies indicated that

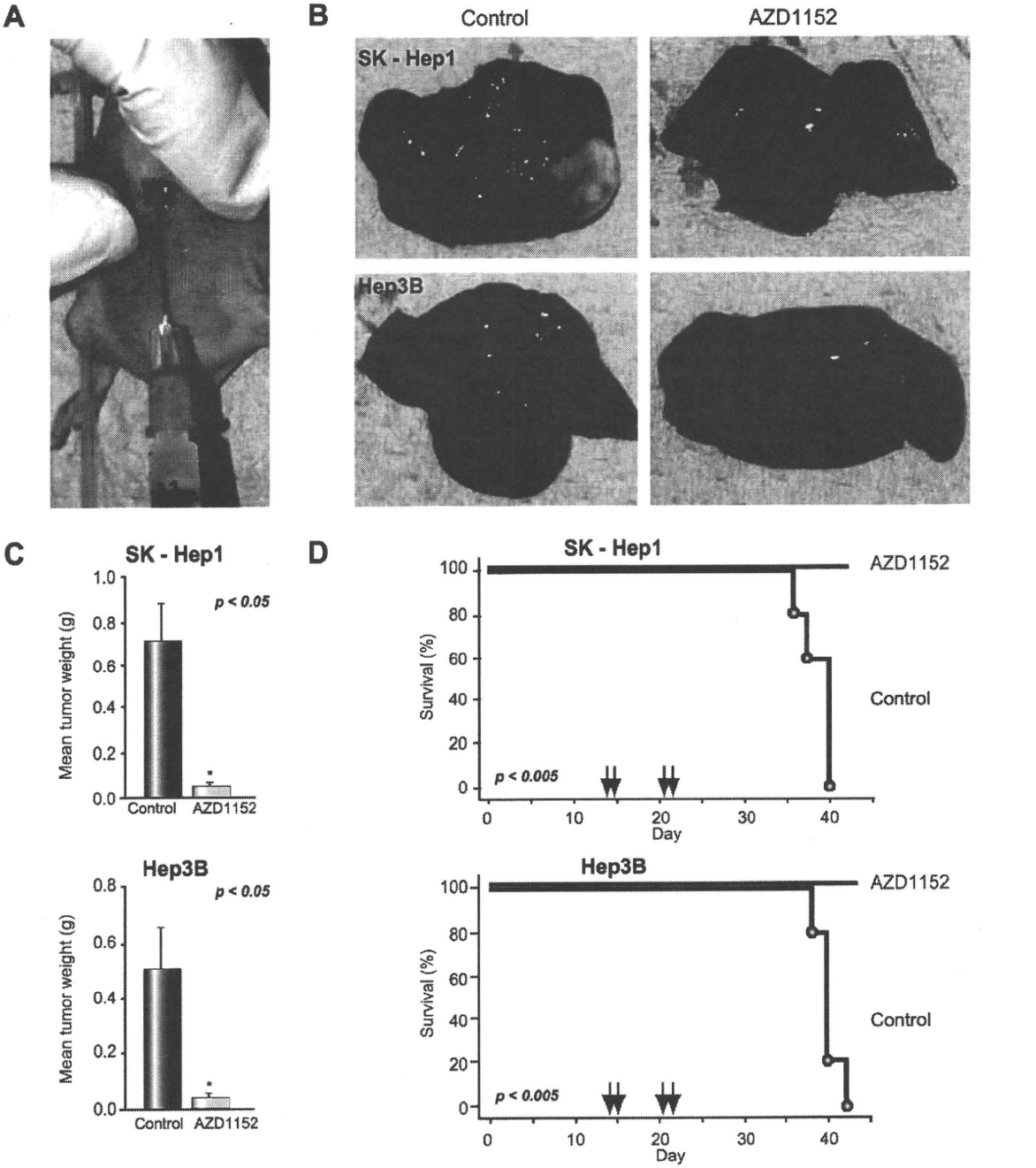

Fig. 5. ***In vivo*** **effects of AZD1152 on human hepatocellular carcinoma (HCC) growth in orthotopic xenograft models.** (A) Schematic representation of generation of orthotopic xenografts. A small transverse incision was made below the sternum to expose the liver, and 2.5×10^6 cells with Matrigel were then slowly injected at a 30° angle into the upper left lobe of the liver using a 28-gauge needle. After 14 days, the mice were treated intraperitoneally with AZD1152 100 mg/kg or the control Tris buffer on 2 consecutive days per week for 2 weeks. (B) The liver tumor in mice within 4 weeks after administration of AZD1152 (light) and the control (right). Cell lines: SK-Hep1 (upper) and Hep3B (lower). (C) Liver tumor weight was analyzed within 4 weeks after administration of AZD1152 or the control ($n = 5$). SK-Hep1 (upper), and Hep3B (lower). Vertical bars, standard error. Statistical analysis was done by two-tailed Student t test ($^*p < 0.05$). (D) Results are expressed in terms of percent survival in experiment time. Arrows, timing of administration. Statistical differences were analyzed by Mantel–Cox log-rank test ($p < 0.005$).

AZD1152, a specific inhibitor of Aurora B kinase, is a promising novel therapeutic approach for the treatment of human HCC. Urgent studies and clinical trials of AZD1152 will confirm its role in the treatment of HCC.

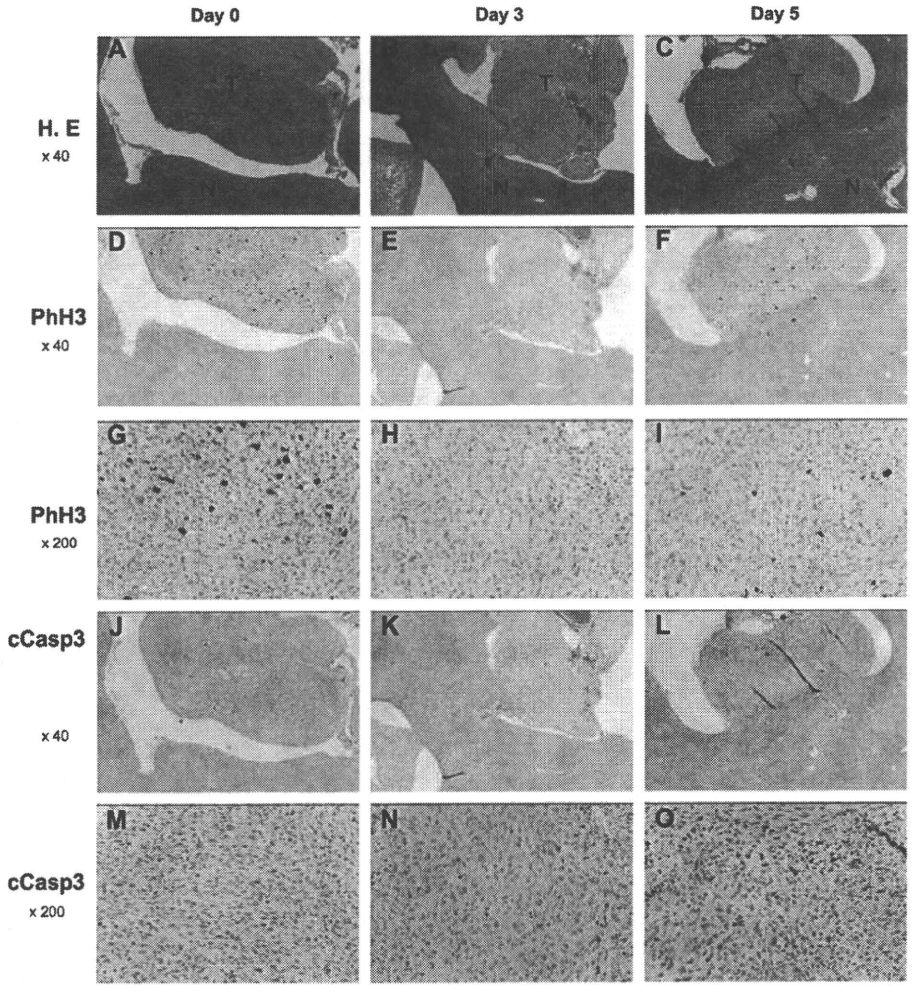

Fig. 6. Pharmacobiological analysis of orthotopic xenograft models. Established orthotopic xenografts of human SK-Hep1 hepatocellular carcinoma (HCC) cells were treated intraperitoneally with AZD1152 100 mg/kg on 2 consecutive days. Mice were sacrificed humanely on day 0 prior to treatment and on days 3 and 5 after the first administration of AZD1152 (left, middle and right, respectively). (A–C) Transverse sections of liver tumor (T) or host normal liver (N) were stained with hematoxylin and eosin (HE; magnification ×40). The same sections were analyzed for expression of phosphohistone H3 (PhH3): (D–F) magnification ×40 and (G–I) magnification ×200. The same sections were also analyzed for the apoptotic marker of cleaved caspase-3 (cCasp-3): (J–L) magnification ×40 and (M–O) magnification ×200.

Acknowledgments

The authors who have taken part in this study declared that they do not have anything to disclose regarding funding from industries or conflict of interest with respect to this manuscript.

This research was supported by the Ministry of Education, Science and Culture, Grant-in-Aid for Scientific Research.

We thank AstraZeneca for kindly providing us with AZD1152 and AZD1152-HQPA for experimental studies. We also thank Drs. Robert Wilkinson, Elizabeth Anderson (AstraZeneca) for helpful discussion, Sarah Mason (Mudskipper Bioscience) for editorial assistance, Kaoru Mogushi for statistical analysis, Akimoto Nimura for technical advice regarding flow cytometry, and Ayumi Shioya for technical assistance.

References

[1] Farazi PA, DePinho RA. Hepatocellular carcinoma pathogenesis: from genes to environment. Nat Rev Cancer 2006;6:674–687.

[2] Ince N, Wands JR. The increasing incidence of hepatocellular carcinoma. N Engl J Med 1999;340:798–799.

[3] Arii S, Yamaoka Y, Futagawa S, Inoue K, Kobayashi K, Kojiro M, et al. Results of surgical and nonsurgical treatment for small-sized hepatocellular carcinomas: a retrospective and nationwide survey in Japan. The Liver Cancer Study Group of Japan. Hepatology 2000;32:1224–1229.

[4] Sherman M. Recurrence of hepatocellular carcinoma. N Engl J Med 2008;359:2045–2047.

[5] Llovet JM, Burroughs A, Bruix J. Hepatocellular carcinoma. Lancet 2003;362:1907–1917.

[6] Llovet JM, Ricci S, Mazzaferro V, Hilgard P, Gane E, Blanc JF, et al. Sorafenib in advanced hepatocellular carcinoma. N Engl J Med 2008;359:378–390.

[7] Zhu AX. Development of sorafenib and other molecularly targeted agents in hepatocellular carcinoma. Cancer 2008;112:250–259.
[8] Tanaka S, Sugimachi K, Maehara S, Harimoto N, Shirabe K, Wands JR. Oncogenic signal transduction and therapeutic strategy for hepatocellular carcinoma. Surgery 2002;131:S142–S147.
[9] Tanaka S, Noguchi N, Ochiai T, Kudo A, Nakamura N, Ito K, et al. Outcomes and recurrence of initially resectable hepatocellular carcinoma meeting Milan criteria: rationale for partial hepatectomy as first strategy. J Am Coll Surg 2007;204:1–6.
[10] Tanaka S, Arii S, Yasen M, Mogushi K, Su NT, Zhao C, et al. Aurora kinase B is a predictive factor for the aggressive recurrence of hepatocellular carcinoma after curative hepatectomy. Br J Surg 2008;95:611–619.
[11] Lee EC, Frolov A, Li R, Ayala G, Greenberg NM. Targeting Aurora kinases for the treatment of prostate cancer. Cancer Res 2006;66:4996–5002.
[12] Bischoff JR, Anderson L, Zhu Y, Mossie K, Ng L, Souza B, et al. A homologue of Drosophila aurora kinase is oncogenic and amplified in human colorectal cancers. EMBO J 1998;17:3052–3065.
[13] Li D, Zhu J, Firozi PF, Abbruzzese JL, Evans DB, Cleary K, et al. Overexpression of oncogenic STK15/BTAK/Aurora A kinase in human pancreatic cancer. Clin Cancer Res 2003;9:991–997.
[14] Smith SL, Bowers NL, Betticher DC, Gautschi O, Ratschiller D, Hoban PR, et al. Overexpression of aurora B kinase (AURKB) in primary non-small cell lung carcinoma is frequent, generally driven from one allele, and correlates with the level of genetic instability. Br J Cancer 2005;93: 719–729.
[15] Tanaka T, Kimura M, Matsunaga K, Fukada D, Mori H, Okano Y. Centrosomal kinase AIK1 is overexpressed in invasive ductal carcinoma of the breast. Cancer Res 1999;59:2041–2044.
[16] Sorrentino R, Libertini S, Pallante PL, Troncone G, Palombini L, Bavetsias V, et al. Aurora B overexpression associates with the thyroid carcinoma undifferentiated phenotype and is required for thyroid carcinoma cell proliferation. J Clin Endocrinol Metab 2005;90:928–935.
[17] Gautschi O, Heighway J, Mack PC, Purnell PR, Lara Jr PN, Gandara DR. Aurora kinases as anticancer drug targets. Clin Cancer Res 2008;14:1639–1648.
[18] Keen N, Taylor S. Aurora-kinase inhibitors as anticancer agents. Nat Rev Cancer 2004;4:927–936.
[19] Macarulla T, Ramos FJ, Tabernero J. Aurora kinase family: a new target for anticancer drug. Recent Patents Anticancer Drug Discov 2008;3:114–122.
[20] Wilkinson RW, Odedra R, Heaton SP, Wedge SR, Keen NJ, Crafter C, et al. AZD1152, a selective inhibitor of Aurora B kinase, inhibits human tumor xenograft growth by inducing apoptosis. Clin Cancer Res 2007;13:3682–3688.
[21] Yang J, Ikezoe T, Nishioka C, Tasaka T, Taniguchi A, Kuwayama Y, et al. AZD1152, a novel and selective aurora B kinase inhibitor, induces growth arrest, apoptosis, and sensitization for tubulin depolymerizing agent or topoisomerase II inhibitor in human acute leukemia cells in vitro and *in vivo*. Blood 2007;110:2034–2040.
[22] Hoshida Y, Villanueva A, Kobayashi M, Peix J, Chiang DY, Camargo A, et al. Gene expression in fixed tissues and outcome in hepatocellular carcinoma. N Engl J Med 2008;359:1995–2004.
[23] Tredan O, Galmarini CM, Patel K, Tannock IF. Drug resistance and the solid tumor microenvironment. J Natl Cancer Inst 2007;99:1441–1454.
[24] Han C, Wu T. Cyclooxygenase-2-derived prostaglandin E2 promotes human cholangiocarcinoma cell growth and invasion through EP1 receptor-mediated activation of the epidermal growth factor receptor and Akt. J Biol Chem 2005;280:24053–24063.
[25] Lu YS, Kashida Y, Kulp SK, Wang YC, Wang D, Hung JH, et al. Efficacy of a novel histone deacetylase inhibitor in murine models of hepatocellular carcinoma. Hepatology 2007;46:1119–1130.
[26] Harrington EA, Bebbington D, Moore J, Rasmussen RK, Ajose-Adeogun AO, Nakayama T, et al. VX-680, a potent and selective small-molecule inhibitor of the Aurora kinases, suppresses tumor growth in vivo. Nat Med 2004;10:262–267.
[27] Soncini C, Carpinelli P, Gianellini L, Fancelli D, Vianello P, Rusconi L, et al. PHA-680632, a novel Aurora kinase inhibitor with potent antitumoral activity. Clin Cancer Res 2006;12:4080–4089.
[28] Tanaka S, Pero SC, Taguchi K, Shimada M, Mori M, Krag DN, et al. Specific peptide ligand for Grb7 signal transduction protein and pancreatic cancer metastasis. J Natl Cancer Inst 2006;98:491–498.
[29] Tanaka S, Sugimachi K, Yamashita Yi Y, Ohga T, Shirabe K, Shimada M, et al. Tie2 vascular endothelial receptor expression and function in hepatocellular carcinoma. Hepatology 2002;35:861–867.
[30] Raskopf E, Dzienisowicz C, Hilbert T, Rabe C, Leifeld L, Wernert N, et al. Effective angiostatic treatment in a murine metastatic and orthotopic hepatoma model. Hepatology 2005;41:1233–1240.
[31] Gizatullin F, Yao Y, Kung V, Harding MW, Loda M, Shapiro GI. The Aurora kinase inhibitor VX680 induces endoreduplication and apoptosis preferentially in cells compromised p53-dependent postmitotic checkpoint function. Cancer Res 2006;66:7668–7677.
[32] Bressac B, Galvin KM, Liang TJ, Isselbacher KJ, Wands JR, Ozturk M. Abnormal structure and expression of p53 gene in human hepatocellular carcinoma. Proc Natl Acad Sci USA 1990;87:1973–1977.
[33] Hsu IC, Tokiwa T, Bennett W, Metcalf RA, Welsh JA, Sun T, et al. P53 gene mutation and integrated hepatitis B viral DNA sequences in human liver cancer cell lines. Carcinogenesis (Lond.) 1993;14:987–992.
[34] Tanaka S, Toh Y, Adachi E, Matsumata T, Mori R, Sugimachi K. Tumor progression in hepatocellular carcinoma may be mediated by p53 mutation. Cancer Res 1993;53:2884–2887.
[35] Mortlock AA, Foote KM, Heron NM, Jung FH, Pasquet G, Lohmann JJ, et al. Discovery, synthesis, and in vivo activity of a new class of pyrazoloquinazolines as selective inhibitors of aurora B kinase. J Med Chem 2007;50:2213–2224.
[36] Hirota T, Lipp JJ, Toh BH, Peters JM. Histone H3 serine 10 phosphorylation by Aurora B causes HP1 dissociation from heterochromatin. Nature 2005;438:1176–1180.
[37] Maret A, Galy B, Arnaud E, Bayard F, Prats H. Inhibition of fibroblast growth factor 2 expression by antisense RNA induced a loss of the transformed phenotype in a human hepatoma cell line. Cancer Res 1995;55:5075–5079.
[38] Giet R, Petretti C, Prigent C. Aurora kinases, aneuploidy and cancer, a coincidence or a real link? Trends Cell Biol 2005;15:241–250.
[39] Hontz AE, Li SA, Lingle WL, Negron V, Bruzek A, Salisbury JL, et al. Aurora A and B overexpression and centrosome amplification in early estrogen-induced tumor foci in the Syrian hamster kidney: implications for chromosomal instability, aneuploidy, and neoplasia. Cancer Res 2007;67:2957–2963.
[40] Warner SL, Bearss DJ, Han H, Von Hoff DD. Targeting Aurora-2 kinase in cancer. Mol Cancer Ther 2003;2:589–595.
[41] Carmena M, Earnshaw WC. The cellular geography of aurora kinases. Nat Rev Mol Cell Biol 2003;4:842–854.
[42] Yao X, Hu JF, Daniels M, Yien H, Lu H, Sharan H, et al. A novel orthotopic tumor model to study growth factors and oncogenes in hepatocarcinogenesis. Clin Cancer Res 2003;9:2719–2726.

Gene Expression Signature of the Gross Morphology in Hepatocellular Carcinoma

Ayano Murakata, MD, Shinji Tanaka, MD, PhD, FACS*, Kaoru Mogushi, PhD†, Mahmut Yasen, MD, PhD†, Norio Noguchi, MD, PhD*, Takumi Irie, MD, PhD*, Atsushi Kudo, MD, PhD*, Noriaki Nakamura, MD, PhD*, Hiroshi Tanaka, PhD†, and Shigeki Arii, MD, PhD**

Objective: To evaluate the gene expression signature of hepatocellular carcinoma (HCC) in relation to the gross morphology.

Background: Eggel's nodular type of HCC is morphologically subclassified into the single nodular (SN) type, the single nodular type with extranodular growth (SNEG), and the confluent multinodular (CM) type, but their biomolecular differences remain unclear.

Methods: The clinicopathological characteristics and genome-wide gene expressions were analyzed in 275 patients with nodular-type HCC (124 SN-type, 91 SNEG-type, and 60 CM-type) who received curative hepatectomy.

Results: Significantly poor prognosis was recognized in CM types in overall survival ($P = 0.0020$) and recurrence-free survival ($P = 0.0066$). Analysis of the genome-wide expression patterns revealed significant difference of CM-type HCC from either SN- or SNEG-type HCC. In particular, a stem cell marker EpCAM was dominantly expressed in CM-type HCC. Immunohistochemical studies confirmed the specific expression of EpCAM in HCC cancer cells of CM type. In multivariate analysis, the gross morphology of CM type was significantly associated with EpCAM expression ($P = 0.0092$), α-fetoprotein ($P = 0.0424$), "lens culinaris agglutinin-reactive fraction of α-fetoprotein" level ($P = 0.0288$), and the portal vein invasion ($P = 0.0150$). Furthermore, EpCAM was predictive for poor prognosis in overall and recurrence-free survivals of patients with CM-type HCC ($P = 0.0082$ and $P = 0.0043$, respectively).

Conclusion: Our studies suggest that the distinct signature of gene expression is closely related to morphological progression in HCC. Especially, EpCAM might play a critical role in the aggressiveness of CM-type HCC.

(*Ann Surg* 2011;253:94–100)

Tumor morphologies have been identified to associate with their malignant properties[1,2] and the differences of gene expression pattern in cancers.[3,4] Analysis of the preoperative morphology might be apparently predictive for the invasive, metastatic, and/or even recurrent potentials after cancer treatment.[1,2,5] Hepatocellular carcinoma (HCC) is known to demonstrate various morphological appearances.[6] In 1901, Eggel[7] established a classical gross classification of HCC morphology into nodular, massive, and diffuse types on the basis of the autopsy data. As modifications for the surgically resectable HCC by Kanai et al,[8] the nodular type has been subclassified into 3 categories of gross appearance: single nodular (SN) type, single nodular type with extranodular growth (SNEG), and confluent multinodular (CM) type, in accordance with the clinicopathological features.[9,10] Indeed, there are many studies indicating that the SN type showed better prognosis but more malignant potentials were recognized in the CM type of HCC.[11–14] Although this gross classification is widely used as one of the prognostic factors after HCC treatment not only for surgical resection[9] but also for chemoembolization[15,16] and ablation therapy,[17] the molecular backgrounds and differences have not been clarified yet.

Genome-wide transcriptional analysis by microarray offers a systematic approach to unfold comprehensive information regarding the gene expression profiles.[18,19] Furthermore, such studies should potentially lead not only to identification of unique biomarkers[20] but also to development of novel molecular targets for therapy.[21] We have previously analyzed gene expression of lethal recurrence of HCC[22] and identified a novel biomarker and targeting molecule.[23] Our present study aimed at seeking gene signatures and biomarkers associated with the morphological appearance of nodular-type HCC. This is the first report of the genome-wide expression profile of HCC morphology as generated from microarray study. Consequently, the molecular features and potential targets for therapy were found with special emphasis on the morphological progression in HCC.

MATERIALS AND METHODS

Subjects and Tissue Samples

Between April 2000 and October 2008, 275 patients with nodular-type HCC underwent curative hepatectomy at the Tokyo Medical and Dental University Hospital. Written informed consent was obtained from each subject, and study procedures were approved by the institutional review board. Preoperative evaluations, including tumor markers α-fetoprotein (AFP), lens culinaris agglutinin-reactive fraction of AFP (AFP-L3), and protein induced by vitamin K absence or antagonists-II (PIVKA-II), were essentially described elsewhere.[22] According to the General Rules for the Clinical and Pathological Study of Primary Liver Cancer by Liver Cancer Study Group of Japan,[24] 275 cases were pathologically subclassified into 124 SN-type, 91 SNEG-type, and 60 CM-type HCCs. The largest area of the lesion was evaluated to determine the gross type. When more than 1 grow type were present, the predominant type (the one with a larger volume) was recorded in this study. The diagnosis was evaluated by 3 independent pathologists. Resected tissues were further analyzed as described previously.[22]

Microarray Analysis of Gene Expression

The tissue preparation was essentially compliant with the General Rules for the Clinical and Pathological Study of Primary Liver Cancer.[24] For the gene expression analysis, at least 3 sections of the largest nodule were used from the largest cross section of the main tumor. Total RNA was extracted from HCC specimens by using an RNeasy kit (Qiagen, Hilden, Germany). The integrity of the obtained RNA (RNA integrity number > 5.0) was confirmed using an Agilent 2100 BioAnalyzer (Agilent Technologies, Palo Alto, Calif). For further analysis of gene expression, 129 samples, 62 SN-type,

From the *Department of Hepato-Biliary-Pancreatic Surgery and †Information Center for Medical Sciences, Tokyo Medical and Dental University, Tokyo, Japan.

No conflicts of interest exist.

Reprints: Shinji Tanaka, MD, PhD, FACS, Department of Hepato-Biliary-Pancreatic Surgery, Tokyo Medical and Dental University, Graduate School of Medicine, 1-5-45 Yushima, Bunkyo-ku, Tokyo 113-8519, Japan. E-mail: shinji.msrg@tmd.ac.jp.

ISSN: 0003-4932/11/25301-0094
DOI: 10.1097/SLA.0b013e3181f9bc00

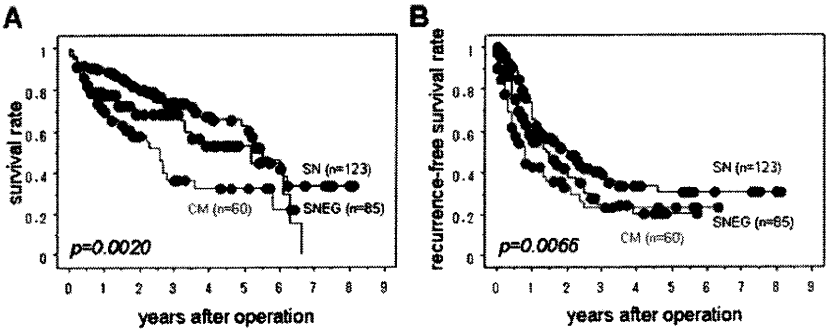

FIGURE 1. Postoperative prognosis of patients with HCC according to the gross morphology of SN, SNEG, and CM types. (A) Overall survival curves and (B) recurrence-free survival curves. Log-rank test demonstrated statistically significant differences in overall and recurrence-free survival rates ($P = 0.0020$ and $P = 0.0066$, respectively).

TABLE 1. The Differentially Expressed Genes in CM-Type HCC by Ranking of the Fold Change (Top 20)

Symbol	Title	*P*	Fold Change
EpCAM	Epithelial cell adhesion molecule (TACSTD1)	1.84E-03	3.43
SLC39A4	Solute carrier family 39 (zinc transporter), member 4	3.24E-05	2.65
CTHRC1	Collagen triple helix repeat containing 1	3.14E-03	2.62
ELOVL7	ELOVL family member 7	8.04E-03	2.37
EPPK1	Epiplakin 1	3.48E-03	2.15
ZNF83	Zinc finger protein 83	1.21E-04	2.14
FOXQ1	Forkhead box Q1	8.49E-03	2.14
NT5DC2	5′-nucleotidase domain containing 2	4.55E-05	2.13
FGFR2	Fibroblast growth factor receptor 2	9.46E-03	2.10
ZNF331	Zinc finger protein 331	1.17E-03	2.03
GTSE1	G-2 and S-phase expressed 1	4.81E-05	1.99
TMED3	Transmembrane emp24 protein transport domain containing 3	4.07E-03	1.99
GLRB	Glycine receptor, β	5.23E-05	1.93
B3GNT5	β-1,3-*N*-acetylglucosaminyltransferase 5	5.14E-03	1.91
—	CDNA FLJ30069 fis, clone ASTRO1000096	3.48E-03	1.89
FADS1/3	Fatty acid desaturase 1/fatty acid desaturase 3	4.58E-03	1.89
DUSP9	Dual specificity phosphatase 9	2.23E-03	1.88
RAP1GAP	RAP1 GTPase activating protein	9.77E-04	1.80
PNMA6A	Paraneoplastic antigen like 6A	6.95E-04	1.80
FAM72A	Gastric cancer upregulated-2/family with sequence similarity 72 A	1.52E-03	1.79

36 SNEG-type, and 31 CM-type HCCs, were available.#12288; Contaminant DNA was removed by digestion with RNase-free DNase (Qiagen). Using 2 μg of total RNA, cRNA was prepared using 1-cycle target labeling and control reagents kit (Affymetrix, Santa Clara, Calif). Hybridization and signal detection of HG-U133 Plus 2.0 arrays (Affymetrix) were performed as per the manufacturer's instructions. Microarray data sets were normalized using a robust multiarray average method under R 2.9.0 statistical software together with a BioConductor package, as previously described.[22]

Profiling Analyses Using Microarray Data

Fold-change (FC) values were calculated using ratios of geometric means of gene expression levels between subtypes for each of the 54,613 probes on the HG-U133 Plus 2.0 array. Genes differently expressed among SN, SNEG, and CM were evaluated by the Kruskal-Wallis test. False discovery rate (FDR) was used to correct multiple comparisons with microarray data analysis. FDR < 30% (equivalent to $P < 0.00056$ in this case) was used as the selection criteria. Using selected probe sets, principal component (PC) analysis was performed to investigate the analogy of gene expression in relation to the 3 gross morphology patterns.[25] Hierarchical clustering with selected genes was also performed on R software by using the Pearson correlation coefficient as a similarity index and a complete linkage method for agglomeration. For visualization, expression intensities were standardized by z scores (mean = 0 and variance = 1) for each probe set. In addition, the gene expression profiles between 2 groups were analyzed by Mann-Whitney U test. The P-value distributions were represented by the number of probe sets with an interval of 0.05 P-value, as essentially described by Boersma et al.[26]

Immunohistochemical Analysis

To validate the protein expression, immunohistochemical analysis was performed on tissue sections. For the tissue analysis, 262 samples, 117 SN-type, 88 SNEG-type, and 57 CM-type HCCs, were available.#12288; Stained using anti-EpCAM (extracellular domain) monoclonal antibody (clone VU-1D9; AbD Serotec, Oxford, United Kingdom) at 1:100 dilutions with PBS containing 1% bovine serum albumin (Sigma), followed by reactions in an automated immunostainer (Ventana XT System) using and a standard DAB detection kit (Ventana). Tissue samples with any staining in the HCC cancer cells were diagnosed as positive, and the others were diagnosed as negative immunohistochemically. The immunostaining was evaluated under a light microscope by 2 independent investigators.

TABLE 2. Univariate Analysis of Clinicopathologic Features According to the Gross Morphology of HCC

	SN (n = 124)	SNEG (n = 91)	CM (n = 60)	*P*
Age, y	66.5 ± 0.8	66.8 ± 0.9	63.9 ± 1.5	0.14
Sex				0.65
Male	93	73	47	
Female	31	18	13	
Background liver				0.32
Normal liver	5	7	3	
Chronic hepatitis	52	47	23	
Liver cirrhosis	67	36	34	
Albumin, g/dL	3.9 ± 0.1	3.7 ± 0.1	3.8 ± 0.1	0.15
Total bilirubin, mg/dL	0.9 ± 0.1	0.9 ± 0.1	0.9 ± 0.1	0.80
PT%	84.8 ± 1.2	83.7 ± 1.2	83.4 ± 1.6	0.71
AFP, ng/mL	686 ± 265	4204 ± 2007	8536 ± 3541	**0.04** (SN vs SNEG)
				0.0019 (SN vs CM)
				0.26 (SNEG vs CM)
AFP-L3, %	11.2 ± 1.8	16.4 ± 2.9	29.8 ± 4.7	0.11 (SN vs SNEG)
				<0.0001 (SN vs CM)
				0.012 (SNEG vs CM)
PIVKAII, mAU/mL	1714 ± 478	6987 ± 2709	14,865 ± 8573	0.05
Tumor size, cm	3.7 ± 0.2	5.1 ± 0.3	5.4 ± 0.5	**0.0001** (SN vs SNEG)
				0.0002 (SN vs CM)
				0.62 (SNEG vs CM)
Tumor differentiation				0.13
Well	21	12	4	
Moderately	64	45	23	
Poorly	34	32	27	
Portal vein invasion				**<0.0001** (SN vs SNEG)
Positive	21	39	39	**<0.0001** (SN vs CM)
Negative	103	52	21	**0.008** (SNEG vs CM)
Hepatic vein invasion				**0.0002** (SN vs SNEG)
Positive	4	18	16	**<0.0001** (SN vs CM)
Negative	120	73	44	0.32 (SNEG vs CM)
Tumor-node-metastatis stage				
I	22	4	4	
II	63	26	10	**<0.0001** (SN vs SNEG)
III	35	34	22	**<0.0001** (SN vs CM)
IVA	4	26	17	0.59 (SNEG vs CM)
IVB	0	1	3	
Surgical procedure				**0.0068** (SN vs SNEG)
Anatomical	72	69	39	0.3673 (SN vs CM)
Nonanatomical	52	22	21	0.1492 (SNEG vs CM)
EpCAM protein				0.5725 (SN vs SNEG)
Positive	28	25	29	**0.0007** (SN vs CM)
Negative	89	63	28	**0.0105** (SNEG vs CM)

The significance of p values in bold.

Statistical Analysis

All quantitative variables in comparison of the 3 groups were assessed by analysis of variance and Student *t* test with the Bonferroni adjustment for multiple comparisons. Chi-square test was used to compare the qualitative variables. After the univariate analysis, the significant variables were further used for the multivariate analysis according to the logistic regression model. Survival curves were constructed using the Kaplan-Meier method and compared with the log-rank test. Cox's proportional-hazards model was used to evaluate the contribution of variables. *P* values of < 0.05 were considered to have statistical significance.

RESULTS

Postoperative Outcomes of Patients With HCC According to the Gross Morphology

The gross morphology of HCC has been reported to relate closely to its malignant properties.[6,9] We first assessed the

postoperative prognosis of 275 patients with nodular-type HCC composed of 124 SN-type, 91 SNEG-type, and 60 CM-type cases. As shown in Figure 1, the gross morphology was significantly associated with the overall survivals and recurrence-free survivals of patients after curative hepatectomy ($P = 0.0020$ and $P = 0.0066$, respectively). The overall and recurrence-free survivals of patients with CM-type HCC were significantly poorer than those with SN type ($P = 0.0004$ and $P = 0.0020$, respectively), but the difference was marginal compared with SNEG type ($P = 0.0971$ and $P = 0.1776$, respectively). Relatively poor prognosis of HCC patients with SNEG type was recognized in comparison with those with SN type ($P = 0.0503$ and $P = 0.0521$, respectively).

Gene Signature of HCC According to the Gross Morphology

Next, genome-wide expression of genes was analyzed using cDNA microarray, followed by evaluation by the Kruskal-Wallis test to compare among the 3 categories. FDR < 30% was utilized as the selection criteria, and then selected 1022 probe sets were further evaluated for PC analysis and hierarchical clustering. Using the selected probe sets, PC analysis was performed to investigate the analogy of gene expression patterns in relation to 3 categories of the gross morphology.[25] Figure 2A demonstrates the scatter spot graphics of the first PC, the second PC, and the third PC. Although SN (black) and SNEG cases (blue) tended to cluster together, most of CM cases (red) were clearly divided from the SN/SNEG cluster. Analysis of hierarchical clustering[22] also showed the distinct pattern of the gene expression in CM cases compared with SN and SNEG cases (Fig. 2B). In addition, based on Mann-Whitney U test to compare between the 2 categories, the P-value distributions were analyzed as described by Boersma et al.[26] Figure 2C demonstrates a significant enrichment of the differentially expressed genes between CM and either SN or SNEG, but not significance between SN and SNEG. The gene signatures of CM-type HCC proved a distinct pattern of expression compared with those of either SN- or SNEG-type HCC.

EpCAM; Specific Expression in CM-type HCC With Clinical Significance

To identify the differentially expressed genes in CM type compared with SN and SNEG types, probe sets satisfied with both $P < 0.01$ by Mann-Whitney U test and FC > 2.0 were further evaluated. As displayed in Table 1 in order of the FC values, a stem cell marker EpCAM (epithelial cell adhesion molecule) was significantly overexpressed in the CM-type HCC. Immunohistochemical validation of EpCAM protein was then performed using 262 tissue samples of HCC. EpCAM protein was mainly distributed on the cellular membrane in HCC cancer cells of 82 samples (31.3%), but not in those of the remaining 180 samples (68.7%), as represented in Figure 3. Substantially, the immunostaining revealed that EpCAM protein was expressed dominantly in 29 (50.9%) of 57 CM-type HCCs, but only in 28 (23.9%) of the 117 SN types and 25 (28.4%) of the 88 SNEG types ($P = 0.0007$; SN vs CM, $P = 0.0105$; SNEG vs CM).

Univariate analysis for the gross morphology of HCC determined the expression of EpCAM protein, serum level of AFP, AFP-L3, tumor size, portal vein invasion, hepatic vein invasion, tumor-node-metastasis (TNM) stage, and surgical procedure as the significant factors of the HCC morphology (Table 2). Next, the multivariate analysis was performed using the logistic regression model. As shown in Table 3, the expression of EpCAM protein ($P = 0.0092$), AFP ($P = 0.0424$), AFP-L3 level ($P = 0.0288$), and the portal vein invasion ($P = 0.0150$) were statistically independent factors of CM-type HCC.

Finally, the prognostic significance of EpCAM expression was evaluated in the patients with HCC in relation to the gross morphology. Although EpCAM expression was not associated with the patient prognosis of SN- and SNEG-type HCC ($P = 0.2193$), the significant relationship was observed between EpCAM expression and the patient prognosis in the CM-type HCC (Fig. 4A; $P = 0.0082$) or the recurrence (Fig. 4B; $P = 0.0043$). Expression of EpCAM protein might play a critical role in progression of the CM-type HCC.

TABLE 3. Multivariate Analysis for Independent Predictors of the Gross Morphology of HCC

	Odds Ratio (95% Confidential Interval)	P
AFP ≥ 100 (ng/mL)	0.360 (0.134–0.966)	**0.0424**
AFP-L3, %	1.020 (1.002–1.038)	**0.0288**
Tumor size, cm	0.981 (0.841–1.145)	0.8095
Portal vein invasion (+)	3.405 (1.268–9.143)	**0.0150**
Hepatic vein invasion (+)	1.683 (0.563–5.027)	0.3515
Tumor-node-metastasis stage		
II	1.480 (0.258–8.498)	0.6599
III	1.911 (0.279–13.108)	0.5099
IVA	1.569 (0.189–13.043)	0.6768
IVB	1.810 (0.046–71.832)	0.7521
Anatomical resection	0.612 (0.250–1.499)	0.2897
EpCAM positive	3.066 (1.319–7.125)	**0.0092**

The significance of p values in bold.

DISCUSSION

Morphological analysis of tumors has been basically used for predicting the virulent potentials.[1–6] In our present study, the gross differences of HCC were significantly associated with the clinicopathological progression, such as AFP, AFP-L3, tumor size, vessel invasion, TNM stage, and surgical procedure in SNEG and/or CM type (Table 2), resulting in poor prognosis in the patient survivals and recurrence-free survivals (Fig. 1). According to the previous reports, the vascular invasion and microscopic intrahepatic metastasis were observed more frequently in SNEG and CM types than in SN type, and that the recurrence-free survivals of SNEG- and CM-type HCC were significantly poor compared with SN-type HCC.[9,13]#12288; Our results were compatible for these studies and indicated the utility of the gross morphology of HCC to prospect for its malignant properties.

Molecular and biological features affecting the morphological phenotypes, however, have not been clarified yet in HCC. In this study, cDNA microarray technique was applied for the comprehensive analysis of gene expression signatures. Using the Kruskal-Wallis test on the microarray data, the PC analysis[25] and the hierarchical clustering[22] revealed that the SN and SNEG cases clustered together, but the CM cases were clearly distinct from the SN/SNEG cluster (Fig. 2A, B). With additional analysis of the P-value distribution using the Mann-Whitney U test,[26] the significance of differential gene expression was recognized between CM and either SN or SNEG, but not between SN and SNEG (Fig. 2C). From perspective of the gene signatures, it is noteworthy that CM-type HCC might involve essentially distinct origins from the SN and SNEG types that can progress serially. As demonstrated in Table 1, various genes were dominantly expressed in the CM-type HCC, including a stem cell marker EpCAM,[27] zinc transporter SLC39A4,[28] secreted extracellular protein CTHRC1,[29] and lipogenic enzyme ELOVL7,[30] that have been reported to overexpress in various malignancies. Our multivariate analysis revealed that EpCAM was one of the statistically independent factors of CM-type HCC (Table 3).

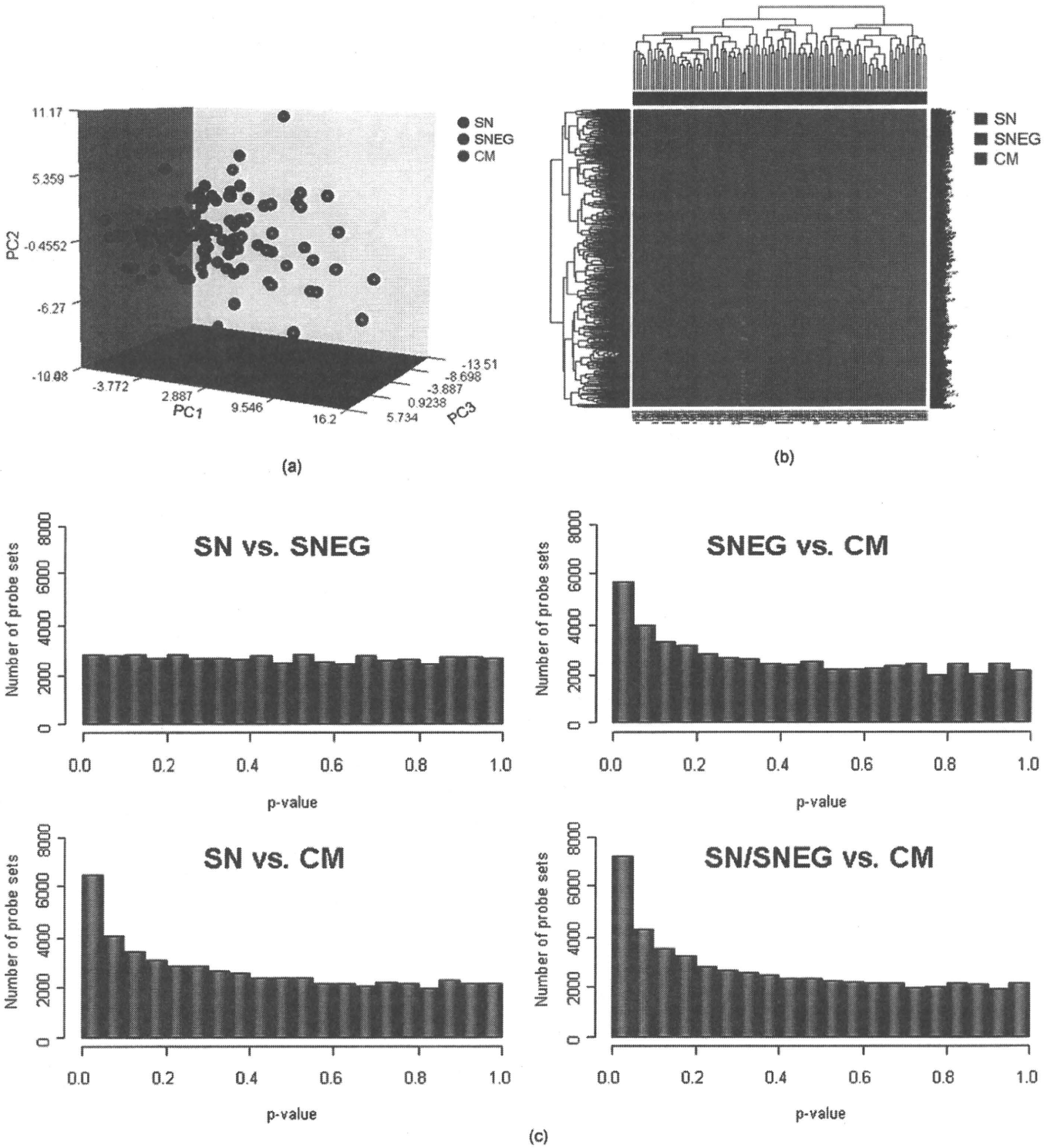

FIGURE 2. Gene expression analysis using cDNA microarray on the gross morphology of HCC. A, Scatter plots from principal component (PC) analysis of gene expression data using the Kruskal-Wallis test. PC1; the first PC, PC2; the second PC, PC3; the third PC. CM cases (red) divided from the cluster of SN (black) and SNEG cases (blue). B, Hierarchical cluster analysis of HCC in relation to the gross morphology. The distinct patterns of the gene expression in CM cases (red) compared with SN (black) and SNEG cases (blue). C, Graphical representation of the *P*-value distribution from Mann-Whitney *U* test for the gross morphology of HCC. The number of differentially expressed probe sets was demonstrated with an interval of 0.05 *P*-value. The significance of differential expression was recognized between CM and either SN or SNEG, but not between SN and SNEG.

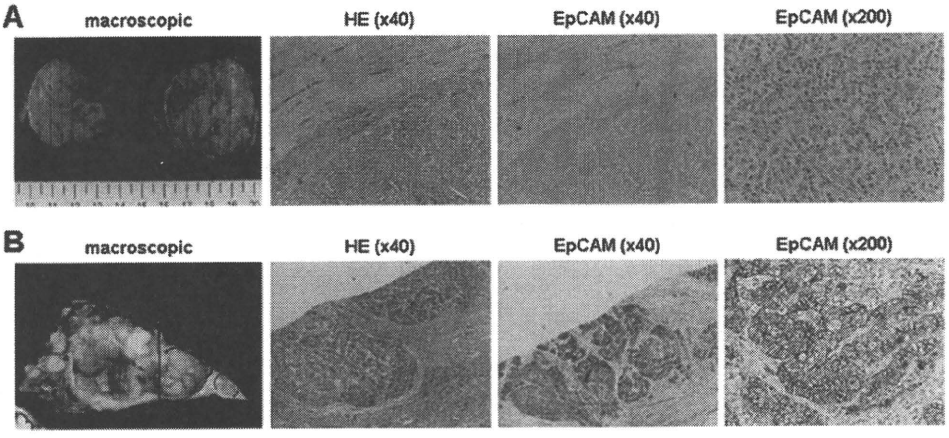

FIGURE 3. Immunohistochemical analysis of EpCAM expression in HCC cases. A, A typical SN morphology showing no EpCAM expression. B, A typical CM morphology showing EpCAM expression. Membranous staining of EpCAM in the cancer cells, but not in the adjacent noncancerous cells (magnification, ×40, ×200). HE; hematoxylin-eosin staining.

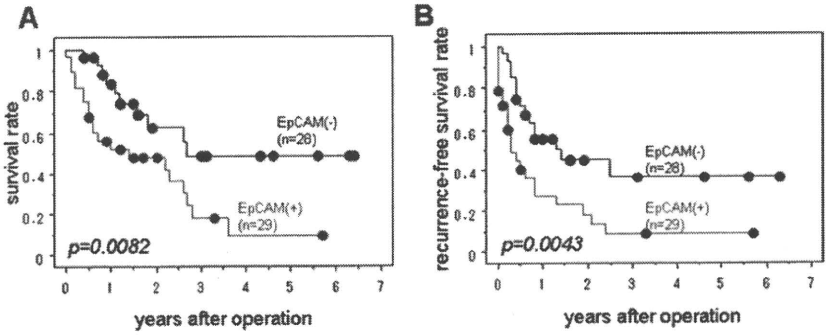

FIGURE 4. Postoperative prognosis of patients with CM-type HCC with (+) or without (−) expression of EpCAM protein. A, Overall survival curves and B, recurrence-free survival curves after curative operation. In the patients with CM-type HCC, EpCAM expression was significantly associated with the poor prognosis after curative operation ($P = 0.0082$ and $P = 0.0044$, respectively).

EpCAM, a type I transmembrane glycoprotein, has been reported to overexpress in various epithelial malignancies[31] and also known as a cancer-specific antigen 17-1A.[32] Gires and colleagues[33] revealed that EpCAM is cleaved by proteolysis on the cancer cell surface to the extracelluar ligand and intracellular domain (ICD).[33,34] The EpCAM-ICD protein directly functions as a transcriptional factor that upregulates c-myc, cyclin A, and cyclin E to promote cell cycling and proliferation.[34] Yamashita et al[35] reported that EpCAM(+)AFP(+) correlated with the poor prognosis in patients with HCC. In our study, however, the expression of EpCAM did not affect the prognosis in patients with high serum level of AFP (data not shown). On the contrary, there is a significant association of EpCAM expression with overall survival and recurrence-free survival in patients with CM-type HCC (Fig. 4; $P = 0.0082$ and $P = 0.0044$, respectively). According to recent studies by Nagrath et al,[36] the EpCAM antigen might be reliable for detection of circulating tumor cells (CTCs), suggesting EpCAM as the useful CTC marker of patients with advanced HCC, especially the CM type. Because more recent studies implied EpCAM as the biomarker for the chemoresistance of HCC,[37] the expression of EpCAM might play multiple roles in cancer progression.

Furthermore, EpCAM known as the cancer-specific antigen 17-1A has been noted as a target molecule for cancer immunotherapy.[38] Clinical trials of monoclonal antibody 17-1A (edrecolomab; Panorex) are ongoing in patients with breast, gastric, colorectal, and ovarian cancers. Recently, a trifunctional bispecific monoclonal antibody catumaxomab (Removab) has been developed for treatment of advanced cancers. Catumaxomab has 2 binding specificities directed at EpCAM and the T-cell antigen CD3, and the recent clinical phase 1/2 trials for patients with peritonea carcinomatosis or malignant pleural effusion showed a promising clinical response.[39,40] Such molecular targeting might be rational for adjuvant therapies of the EpCAM-positive HCC with CM-type.[41] Our present studies suggested not only the distinct gene signature in the CM morphology of HCC but also potentially therapeutic strategy for the aggressive phenotype in the future. Further examinations should be required to elucidate the biological significance of CM-type origination in hepatocarcinogenesis.

REFERENCES

1. Michelassi F, Vannucci L, Montag A, et al. Importance of tumor morphology for the long term prognosis of rectal adenocarcinoma. *Am Surg*. 1988;54(6):376–379.
2. Stahel RA. Morphology, surface antigens, staging, and prognostic factors of small cell lung cancer. *Curr Opin Oncol*. 1992;4(2):308–314.
3. Machado JC, Soares P, Carneiro F, et al. E-cadherin gene mutations provide a genetic basis for the phenotype divergence of mixed gastric carcinomas. *Lab Invest*. 1999;79:459–465.
4. Jaeger J, Koczan D, Thiesen HJ, et al. Gene expression signatures for tumor progression, tumor subtype, and tumor thickness in laser-microdissected melanoma tissues. *Clin Cancer Res*. 2007;13(3):806–815.
5. Montironi R, Cheng L, Lopez-Beltran A, et al. Decision support systems for morphology-based diagnosis and prognosis of prostate neoplasms: a methodological approach. *Cancer*. 2009;115(13)(Suppl):3068–3077.
6. Yang LY, Fang F, Ou DP, et al. Solitary large hepatocellular carcinoma: a specific subtype of hepatocellular carcinoma with good outcome after hepatic resection. *Ann Surg*. 2009;249(1):118–123.
7. Eggel H. Ueber das primare carcinoma der leber. *Beitz Pathol Anat*. 1901;30:506–604.
8. Kanai T, Hirohashi S, Upton MP, et al. Pathology of small hepatocellular carcinoma. A proposal for a new gross classification. *Cancer*. 1987;60:810–819.
9. Hui AM, Takayama T, Sano K, et al. Predictive value of gross classification of hepatocellular carcinoma on recurrence and survival after hepatectomy. *J Hepatol*. 2000;33:975–979.
10. Desmet VJ. East–West Pathology agreement on precancerous liver lesions and early hepatocellular carcinoma. *Hepatology*. 2009;49:355–357.

11. Choi GH, Han DH, Kim DH, et al. Outcome after curative resection for a huge (>10 cm) hepatocellular carcinoma and prognostic significance of gross tumor classification. *Am J Surg*. 2009;198(5):693–701.
12. Shimada M, Rikimaru T, Hamatsu T, et al.The role of macroscopic classification in nodular-type hepatocellular carcinoma. *Am J Surg*. 2001;182: 177–182.
13. Inayoshi J, Ichida T, Sugitani S, et al. Gross appearance of hepatocellular carcinoma reflects E-cadherin expression and risk of early recurrence after surgical treatment. *J Gastroenterol Hepatol*. 2003;18:673–677.
14. Nagano Y, Shimada H, Takeda K, et al. Predictive factors of microvascular invasion in patients with hepatocellular carcinoma larger than 5 cm. *World J Surg*. 2008;32(10):2218–2222.
15. Nakamura H, Liu T, Hori S, et al. Response to transcatheter oily chemoembolization in hepatocellular carcinoma 3 cm or less: a study in 50 patients who underwent surgery. *Hepatogastroenterology*. 1993;40(1):6–9.
16. Hashimoto T, Nakamura H, Hori S, et al. Hepatocellular carcinoma: efficacy of transcatheter oily chemoembolization in relation to macroscopic and microscopic patterns of tumor growth among 100 patients with partial hepatectomy. *Cardiovasc Intervent Radiol*. 1995;18(2):82–86.
17. Yamakado K, Nakatsuka A, Ohmori S, et al. Radiofrequency ablation combined with chemoembolization in hepatocellular carcinoma: treatment response based on tumor size and morphology. *J Vasc Interv Radiol*. 2002;13(12):1225–1232.
18. Quackenbush J. Microarray analysis and tumor classification. *N Engl J Med*. 2006;354 (23):2463–2472.
19. Iizuka N, Oka M, Yamada-Okabe H, et al. Oligonucleotide microarray for prediction of early intrahepatic recurrence of hepatocellular carcinoma after curative resection. *Lancet*. 2003;361 (9361):923–929.
20. Hoshida Y, Villanueva A, Kobayashi M, et al. Gene expression in fixed tissues and outcome in hepatocellular carcinoma. *N Engl J Med*. 2008;359(19):1995–2004.
21. Bild AH, Potti A, Nevins JR. Linking oncogenic pathways with therapeutic opportunities. *Nat Rev Cancer*. 2006;6 (9):735–741.
22. Tanaka S, Arii S, Yasen M, et al. Aurora kinase B is a predictive factor for aggressive recurrence of hepatocellular carcinoma after curative hepatectomy. *Br J Surg*. 2008;95 (5):611–619.
23. Aihara A, Tanaka S, Yasen M, et al. The selective Aurora B kinase inhibitor AZD1152 as a novel treatment for hepatocellular carcinoma. *J Hepatol*. 2010;52(1):63–71.
24. Liver Cancer Study Group of Japan. *The General Rules for the Clinical and Pathological Study of Primary Liver Cancer*. Tokyo, Japan: Kanehara; 1992.
25. Hilsenbeck SG, Friedrichs WE, Schiff R, et al. Statistical analysis of array expression data as applied to the problem of tamoxifen resistance. *J Natl Cancer Inst*. 1999;91(5):453–459.
26. Boersma BJ, Reimers M, Yi M, et al. A stromal gene signature associated with inflammatory breast cancer. *Int J Cancer*. 2008;122 (6): 1324–1332.
27. Schmelzer E, Zhang L, Bruce A, et al. Human hepatic stem cells from fetal and postnatal donors. *J Exp Med*. 2007;204:1973–1987.
28. Li M, Zhang Y, Liu Z, et al. Aberrant expression of zinc transporter ZIP4 (SLC39A4) significantly contributes to human pancreatic cancer pathogenesis and progression. *Proc Natl Acad Sci USA*. 2007;104(47):18636–18641.
29. Tang L, Dai DL, Su M, et al. Aberrant expression of collagen triple helix repeat containing 1 in human solid cancers. *Clin Cancer Res*. 2006;12(12):3716–3722.
30. Tamura K, Makino A, Hullin-Matsuda F, et al. Novel lipogenic enzyme ELOVL7 is involved in prostate cancer growth through saturated long-chain fatty acid metabolism. *Cancer Res*. 2009;69(20):8133–8140.
31. Trzpis M, McLaughlin PMJ, Leij LMFH, et al. Epithelial cell adhesion molecule. More than a carcinoma marker and adhesion molecule. *Am J Pathol*. 2007;171:386–395.
32. Went P, Vasei M, Bubendorf L, et al. Frequent high-level expression of the immunotherapeutic target EpCAM in colon, stomach, prostate and lung cancers. *Br J Cancer*. 2006;94:128–135.
33. Mastzel D, Denzel S, Mack B, et al. Nuclear signaling by tumor-associated antigen EpCAM. *Nat Cell Biol*. 2009;11:162–171.
34. Munz M, Baeuerle PA, Gires O. The emerging role of EpCAM in cancer and stem cell signaling. *Cancer Res*. 2009;69(14):5627–5629.
35. Yamashita T, Forgues M, Wang W, et al. EpCAM and α-fetoprotein expression defines novel prognostic subtypes of hepatocellular carcinoma. *Cancer Res*. 2008;68:1451–1461.
36. Nagrath S, Sequist LV, Maheswaran S, et al. Isolation of rare circulating tumour cells in cancer patients by microchip technology. *Nature*. 2007;450(7173):1235–1239.
37. Noda T, Nagano H, Takemasa I, et al. Activation of Wnt/beta-catenin signalling pathway induces chemoresistance to interferon-alpha/5-fluorouracil combination therapy for hepatocellular carcinoma. *Br J Cancer*. 2009;100:1647–1658.
38. Chaudry MA, Sales K, Ruf P, et al. EpCAM an immunotherapeutic target for gastrointestinal malignancy: current experience and future challenges. *Br J Cancer*. 2007;96:1013–1019.
39. Ströhlein MA, Siegel R, Jäger M, et al. Induction of anti-tumor immunity by trifunctional antibodies in patients with peritonea carcinomatosis. *J Exp Clin Cancer Res*. 2009;28:18.
40. Sebastian M, Kiewe P, Schuette W, et al. Treatment of malignant pleural effusion with the trifunctional antibody catumaxomab (Removab) (anti-EpCAM x Anti-CD3): results of a phase 1/2 study. *J Immunother*. 2009;32 (2):195–202.
41. Tanaka S, Arii S. Molecularly targeted therapy for hepatocellular carcinoma. *Cancer Sci*. 2009;100(1):1–8.

Review Article

Molecularly targeted therapy for hepatocellular carcinoma

Shinji Tanaka[1] and Shigeki Arii

Department of Hepato-Biliary-Pancreatic Surgery, Tokyo Medical and Dental University, Yushima 1-5-45, Bunkyo-ku, Tokyo 113-8519, Japan

(Received July 30, 2008/Revised September 5, 2008/Accepted September 8, 2008/Online publication November 25, 2008)

Accumulated understanding of the molecular pathways regulating cancer progression has led to the development of novel targeted therapies. Hepatocellular carcinoma (HCC) remains a highly lethal disease that is resistant to conventional cytotoxic chemotherapy and radiotherapy. Unlike conventional chemotherapy, molecular-targeted agents offer the potential advantages of a relatively high therapeutic window and use in combination with other anticancer strategies without overlapping toxicity. It is hoped that these drugs will become valuable therapeutic tools within the multimodal approach to treating cancer. A recent clinical trial revealed an oral multikinase inhibitor, sorafenib, as the first agent that has demonstrated improved overall survival in patients with advanced HCC. The present review summarizes molecular abnormalities of HCC with a focus on clinical studies, and current status as well as problems of the targeted strategies for HCC. (*Cancer Sci* 2009; 100: 1–8)

Hepatocellular carcinoma (HCC) is one of the most common malignancies worldwide accounting for 500 000–600 000 deaths per year,[1,2] and the incidence is still increasing.[3] Although the primary curative treatment for HCC is surgical resection, there has been limited improvement in the availability of alternative treatments in the last decade.[4] A major obstacle for the treatment of HCC is the high frequency of tumor recurrence after curative resection. In fact, effective palliative treatment is hindered by the fact that HCC is frequently resistant to conventional chemotherapy and radiotherapy.[4] Moreover, the existing conventional chemotherapeutics are more or less non-selective cytotoxic drugs with significant systemic side effects. Importantly, as most patients with HCC have compromised liver function aggressive medical therapy regimens can not be applied. Thus, usually no effective therapy can be offered to these patients.[2,4] There is an urgent need to develop novel treatments for recurrent and advanced HCC.

Numerous studies on molecular abnormalities in HCC progression have revealed the crucial roles of such molecules in cell proliferation, as well as survival not only of cancer cells but also angiogenic or stromal cells.[5,6] Among the key pathways in the pathogenesis of HCC, this review focuses on the pathological processes including vascular endothelial growth factor (VEGF)-dependent tumor angiogenesis, epidermal growth factor receptor (EGFR), and insulin-like growth factor (IGF)-dependent tumor cell proliferation and survival in HCC (Fig. 1). Furthermore, several intracellular factors essential for hepatocarcinogenesis are demonstrated (Figs 2,3), coupled with molecularly targeted agents in clinical trials (Table 1).

VEGF and VEGF receptor family

In vivo tumor progression requires various host factors as well as tumor factors; in particular, neovascularization is one of the most important host factors.[7] HCC is well known as one of the tumors to present with typical neovascularization. A dramatic alteration in the arterial hypervascularity is observed in moderately to poorly differentiated-type HCC, but the new blood vessels are so irregular that the flow is often stagnated.[7,8] VEGF is one of the most potent growth factors of the vascular endothelial cells, as well as one of the critical effectors on progenitor cells.[9] The VEGF ligand family consists of VEGF-A, VEGF-B, VEGF-C, VEGF-D, PIGF-1, PIGF-2, and VEGF-E derived from a virus gene (Fig. 1a).[10] VEGF-A and VEGF-B have spliced variants. The currently known VEGF genes and polypeptides belong to a family of structurally and functionally related growth factors, which also includes the platelet-derived growth factors (PDGF) that mainly function in the vascular mural cells (pericytes). In *Drosophila*, PEGF and VEGF-like factors share a single receptor. The human VEGF receptor (VEGFR) family consists of VEGFR-1/Flt-1, VEGFR-2/KDR/Flk-1, and VEGFR-3/Flt-4. Although either VEGFR-1 or VEGFR-2 regulates angiogenesis and vasculogenesis, VEGFR-3 is mainly related to lymphoangiogenesis.[11] We first found a close relationship between VEGF expression and the vascularity of HCC tumors compared that of non-cancerous liver tissue from a clinical specimen.[12] The expression of VEGF protein was found to correlate with clinicopathological factors such as proliferation, vascular invasion, and tumor multiplicity.[13] VEGF expression was reported to associate with not only invasion and metastasis of HCC,[14] but also postoperative recurrence.[15]

Expression of VEGF is regulated by micro-environmental and genetic alterations in cancer cells. Hypoxia is a key micro-environmental factor of angiogenesis, and hypoxia-inducible factors (HIF) are known to stimulate VEGF expression.[16,17] The upregulation of VEGF in HCC is controlled by transcriptional levels as well as the mRNA stability of VEGF.[18] In addition, the *p53* tumor-suppressor and *HBx* genes might regulate VEGF expression in HCC.[19,20] Furthermore, we previously identified angiopoietin-2–Tie2 signaling as another angiogenic pathway essential for HCC progression.[9,21] These angiopoietin-2 signals also require VEGF activation in the angiogenic switch.[22]

It should be mentioned that the receptors VEGFR-1/Flt-1 and VEGFR-2/KDR/Flk-1 have been identified on HCC cells.[23] These findings suggest that VEGF might function in the migration of endothelial cells, as well as in HCC cells per se, indicating a possibly novel mechanism for HCC progression.[24] Recent studies revealed critical roles of VEGFR-1-expressing hematopoietic cells in formation of the premetastatic niche.[25,26] VEGF signaling functions not only in angiogenesis but also in cancer invasion and metastasis.[27] Given that the VEGF and VEGFR pathways are required for the pathogenesis and progression of HCC, it is

[1]To whom correspondence should be addressed. E-mail: shinji.msrg@tmd.ac.jp

doi: 10.1111/j.1349-7006.2008.01006.x

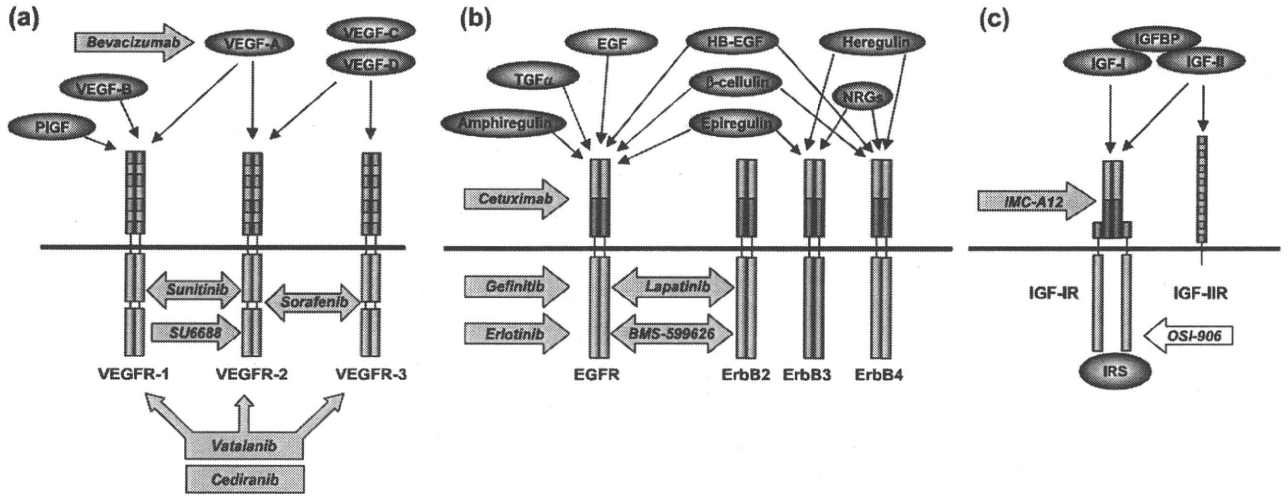

Fig. 1. Molecular targets in the (a) epidermal growth factor (EGF) and EGF receptor (EGFR) family, (b) vascular endothelial growth factor (VEGF) and VEGF receptor (VEGFR) family, and (c) insulin-like growth factor (IGF) and IGF receptor (IGFR). Targeted agents are indicated by arrows.

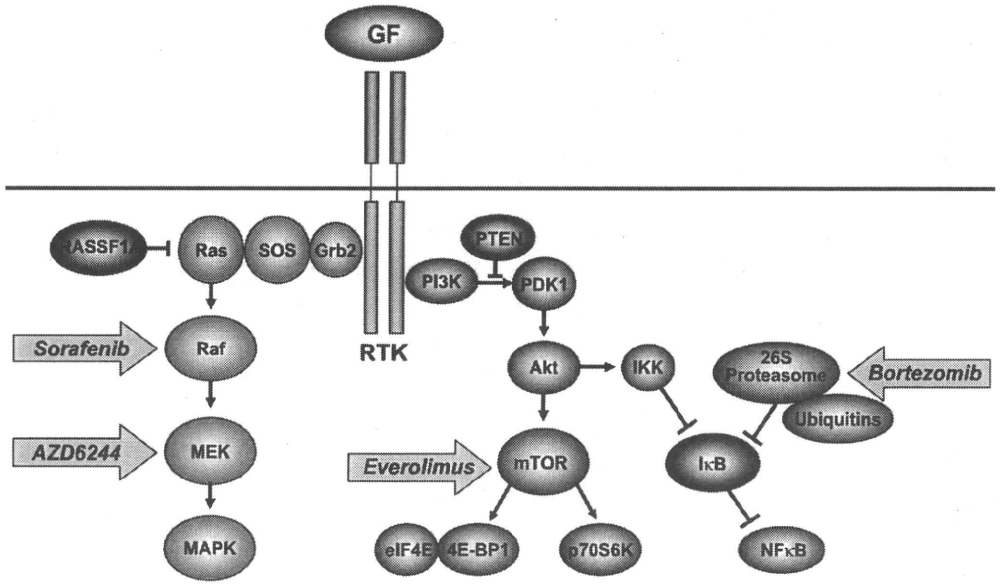

Fig. 2. Molecular targets in mitogen-activated protein kinase (MAPK) and phosphatidylinositol-3 kinase (PI3K) signal transduction pathways stimulated by receptor tyrosine kinases (RTK). Targeted agents are indicated by arrows. GF, growth factor; SOS, sun of sevenless; MEK, MAPK/extracellular regulated kinase kinase; PTEN, phospharase and tensin homologue; PDK, phosphoinositide-dependent kinase; IKK, IκB kinase; mTOR, mammalian target of rapamycin.

possible that inhibitors of VEGF signaling are promising therapeutic agents for HCC treatment.

Most of these compounds can be broadly classified into two main categories: small-molecule kinase inhibitors and monoclonal antibodies. Sorafenib (Nexavar, BAY43-9006) is a unique multitargeting small molecule that inhibits the receptor tyrosine kinases (RTK) VEGFR-2, VEGFR-3, Flt-3, PDGF receptor (PDGFR), and fibroblast growth factor receptor (FGFR)-1, as well as Raf serine-threonine kinase in the signal transduction pathway Ras–Raf–mitogen-activated protein kinase/extracellular regulated kinase (MEK) –mitogen-activated protein kinase (MAPK)[28] (Figs 1a,2). In a recent phase III trial, the Sorafenib HCC Assessment Randomized Protocol (SHARP), 602 patients with advanced HCC who had received no prior systemic therapy were evaluated and randomized to receive either sorafenib ($n = 299$) or placebo ($n = 303$).[1] The median overall survival was 10.7 months in sorafenib-treated patients compared with 7.9 months in patients who received placebo, indicating a 44% increase in overall survival (hazard ratio, 0.69; $P < 0.0001$). The median time to radiological progression was 5.5 months in sorafenib-treated patients compared with 2.8 months in patients who received placebo (hazard ratio, 0.58; $P < 0.0001$). The overall incidence of treatment-related adverse events was 80% in the sorafenib group and 52% in the placebo group. Grade 3 drug-related adverse events included diarrhea (8% in the sorafenib group vs 2% in the placebo group, $P < 0.001$), and hand or foot skin reaction (8% in the sorafenib group vs <1% in the placebo group, $P < 0.001$). Grade 3 or 4 laboratory abnormalities occurred with grade 3 hypophosphatemia (11% in the sorafenib group vs 2% in the placebo group, $P < 0.001$) and grade 3 or 4 thrombocytopenia

doi: 10.1111/j.1349-7006.2008.01006.x

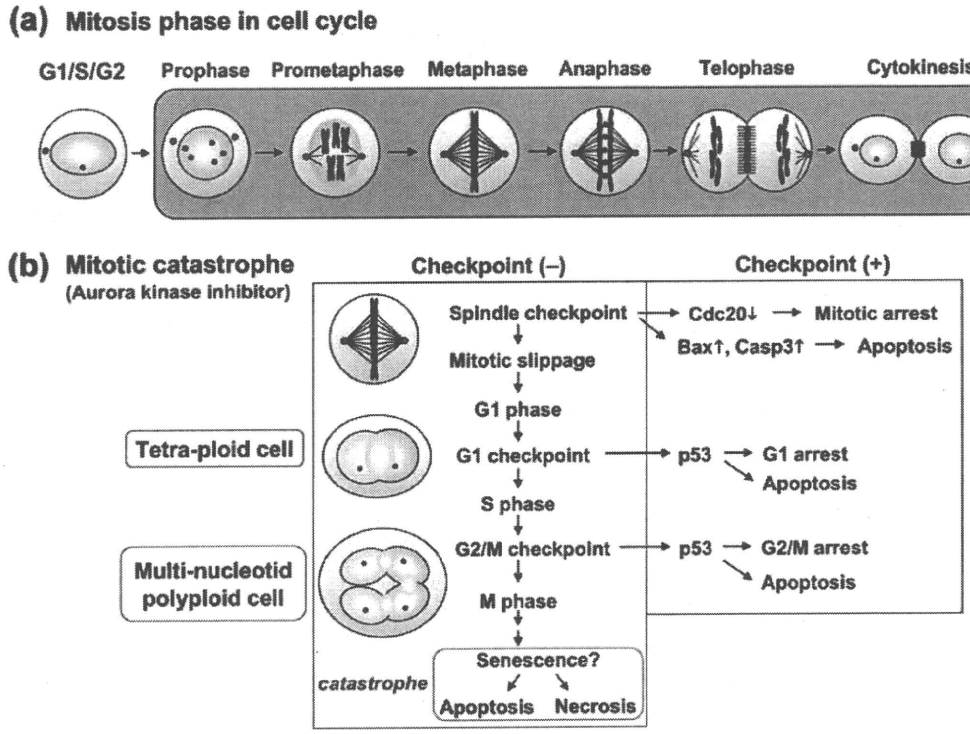

Fig. 3. (a) The mitosis phase of the cell cycle. Localization of Aurora kinases is shown. Green spots, the centrosome protein Aurora kinase A; red spots, the chromosomal passenger Aurora kinase B. (b) The concept of mitotic catastrophe, induced by inhibition of Aurora kinases in cancer cells. Under abnormalities in each checkpoint system, p53-independent death is induced as senescence-like polyploidy without successfully completing mitosis.

Table 1. Molecularly targeted agents for hepatocellular carcinoma

Agent	Classification	Function	Clinical trial
Sorafenib (Nexabar, BAY43-9006)	Small molecule compound	VEGFR2, VEGFR3, PDGFR-β tyrosine kinase, Raf serine/threonine kinase inhibitor	Phase III
Sunitinib (Sutent, SU11248)	Small molecule compound	VEGFR1, VEGFR2, PDGFR, Flt-3, c-KIT tyrosine kinase inhibitor	Phase II
SU6688 (TSU-68)	Small molecule compound	VEGFR2, PDGF R-β, FGFR tyrosine kinase inhibitor	Phase II
Vatalanib (PTK787/ZK222584)	Small molecule compound	VEGFR1, VEGFR2, VEGFR3, PDGFR-β, c-KIT tyrosine kinase inhibitor	Phase II
Cediranib (AZD2171)	Small molecule compound	VEGFR1, VEGFR2, VEGFR3, PDGFR, c-KIT tyrosine kinase inhibitor	Phase II
Bevacizumab (Avastin)	Monoclonal antibody	VEGF-A neutralization	Phase II
Gefintinib (Iressa, ZD1839)	Small molecule compound	EGFR/ErbB1/Her1 tyrosine kinase inhibitor	Phase II
Erlotinib (Tarceva, OSI774)	Small molecule compound	EGFR/ErbB1/Her1 tyrosine kinase inhibitor	Phase II
Lapatinib (Tykerb, GW572016)	Small molecule compound	EGFR/ErbB1/Her1 and ErbB2/Her2/Neu tyrosine kinase inhibitor	Phase II
BMS-599626	Small molecule compound	EGFR/ErbB1/Her1 and ErbB2/Her2/Neu tyrosine kinase inhibitor	Phase II
Cetuximab (Erbitux, GW572016)	Monoclonal antibody	EGFR/ErbB1/Her1 neutralization	Phase II
AZD6244 (ARRY-142886)	Small molecule compound	MEK serine-threonine tyrosine kinase inhibitor	Phase II
IMC-A12	Monoclonal antibody	IGF-IR neutralization	Phase II
Everolimus (RAD001)	Small molecule compound	mTOR serine-threonine kinase inhibitor	Phase I and II
Sirolimus (Rapamune)	Small molecule compound	mTOR serine-threonine kinase inhibitor	Phase I
Bortezomib (Velcade)	Small molecule compound	Proteasome inhibitor	Phase I and II
PXD101 (Belinostat)	Small molecule compound	HDAC inhibitor	Phase I and II
PI-88	Small molecule compound	Heparanase inhibitor	Phase III

(4% in the sorafenib group vs <1% in the placebo group, $P = 0.006$).

Sunitinib (Sutent, SU11248) is another oral inhibitor that targets RTK of the split-kinase domain family, including VEGFR-1, VEGFR-2, PDGFR-α, PDGFR-β, c-Kit, Flt-3, and RET.[29] The phase II studies have examined the tolerability and efficacy of sunitinib in patients with advanced HCC.[30] Of the 37 patients enrolled, one patient had a confirmed partial response (PR), and 39% patients had stable disease (SD) as their best response. Grade 3 and 4 toxicities included thrombocytopenia (43%), neutropenia (24%), central nervous system symptoms (24%), asthenia (22%), and hemorrhage (14%). Dose reductions were required in 27%

patients. Four patients developed grade 5 events, including ascites, edema, bleeding, drowsiness, and hepatic encephalopathy.

Vatalanib (PTK787/ZK222584) is an oral pan-VEGFR inhibitor with activity against PDGFR-β and c-Kit (Fig. 1a).[31] Preclinical studies suggested anti-angiogenic and angiogenesis-independent effects on HCC growth arrest.[32] In a phase I study of vatalanib in 18 patients with unresectable HCC, nine patients had a best response of SD, and nine patients had progressive disease (PD).[33] Cediranib (AZD2171) is another potent pan-VEGFR inhibitor with activity against PDGFR and c-Kit.[34] According to a phase II study of cediranib in patients with advanced HCC, 28 patients were accrued, and 19 patients were evaluable for toxicity.[35] Of these, 16 patients (84%) developed grade 3 toxicity. Fatigue, hypertension, and anorexia accounted for the majority of adverse events. A high rate of refusal of further treatment was encountered and apparently was related to the high rate of grade 3 fatigue. A dose reduction of cediranib was planned in an ongoing study. SU6668 (TSU-68) is a potent RTK inhibitor against VEGFR-2, PDGFR-β, and FGFR.[36] According to preliminary data from a Japanese phase I and II study in 15 HCC patients, one patient had PR, seven patients had SD (two patients for over 12 months), and seven patients had PD.[37] Tumor necrosis was observed in eight patients. The adverse events were hypoalbuminemia, diarrhea, abdominal pain, fever, and aspartate aminotransferase (AST) and alanine aminotransferase (ALT) elevation.

Bevacizumab (Avastin), a recombinant, humanized monoclonal antibody that targets VEGF, has emerged as an important therapeutic agent in several malignancies.[38] In addition to its direct antiangiogenic effects, bevacizumab may enhance chemotherapy administration by normalizing tumor vasculature.[39] Several studies have explored the use of bevacizumab either as a single agent or in combination with cytotoxic or molecularly targeted agents in patients with HCC. In a phase I study in 25 patients using single-agent bevacizumab, two patients had a PR, and 18 patients had SD. The median time to progression was 6.5 months.[40] In a phase II study using single-agent bevacizumab,[41] among the 24 patients who were evaluable for efficacy, three patients had a PR and seven patients had SD that lasted at least 16 weeks. The combination of bevacizumab with cytotoxic agents also was evaluated. In a recent phase II study, bevacizumab in combination with gemcitabine and oxaliplatin (GEMOX) was used as treatment for patients with advanced HCC.[42] This regimen had moderate antitumor activity in HCC with an overall response rate of 20% in evaluable patients. An additional 27% patients had SD with a median duration of 9 months. The median overall survival was 9.6 months, the median progression-free survival was 5.3 months, and the progression-free survival rate at 3 and 6 months approached 70 and 48%, respectively. Bevacizumab-related side effects, including hypertension, bleeding, and proteinuria, were generally manageable. The encouraging results from that early study should be confirmed cautiously by an independent study in the future.

EGFR/ErbB family

EGFR/ErbB1/Her1 is a member of a RTK family that also includes ErbB2/Her2/Neu, ErbB3/Her3, and ErbB4/Her4 (Fig. 1b).[43] EGFR/ErbB1 binds not only epidermal growth factor (EGF) but also transforming growth factor (TGF)-α, amphiregulin, HB-EGF, β-cellulin, and epiregulin. Although heregulins, epiregulin, and NRG have been identified as ligands of ErbB3/Her3, and heregulins, epiregulin, HB-EGF, β-cellulin, and NRG have been identified as ligands of ErbB4/Her4, no ligands have been identified for ErbB2/Her2/Neu. Either EEGFR/ErbB1 or ErbB2/Her2/Neu is overexpressed in various cancers. The binding of ligand to EGFR/ErbB1 leads to homodimerization or heterodimerization with ErbB2/Her2/Neu or ErbB3/Her3, resulting in tyrosine kinase activation and self-phosphorylation (not in ErbB2/Her3). Activation of RTK transduces the MAPK and phosphatidylinositol-3 kinase (PI3K) signaling pathways. The MAPK signals mainly stimulate cell proliferation, and the PI3K signals activate Akt anti-apoptotic pathways. Overexpression of TGF-α has been observed in the early stages of hepatocarcinogenesis, and is associated with upregulation of VEGF.[44]

The crucial role of EGFR in HCC proliferation has provided the rationale for targeting and interrupting this key signaling network. Gefinitib (Iressa, ZD1839) is an oral tyrosine kinase inhibitor that selectively suppresses EGFR and not other tyrosine kinases such as ErbB2 or VEGFR (Fig. 1).[45] According to the clinical trials for non-small lung cancers, the effects of gefitinib correlate with EGFR mutations in cancer cells.[46,47] In a phase II clinical trial of 31 patients with HCC, one patient had PR and seven patients had SD, but there were no clear effects using single administration as the median overall survival was 6.5 months and the median progression-free survival was 2.8 months.[48] The criterion for second-stage accrual was not met, and the authors concluded that gefitinib as a single agent was not active in patients with advanced HCC. Erlotinib (Tarceva, OSI774) is another oral EGFR-selective inhibitor, and two phase II clinical studies have evaluated its safety and efficacy in patients with advanced HCC.[49] In the study by Philip *et al.*, 3 of 38 patients had PR and 12 patients had progression-free survival at 6 months.[50] The median overall survival for this cohort was 13 months. In another report by Thomas *et al.* 17 of 40 patients achieved progression-free survival at 16 weeks and the progression-free survival rate at 24 weeks was 28%.[51] No PR or complete response (CR) was observed in that study, but the median overall survival was 25 weeks. Lapatinib (Tykerb, GW572016), a selective dual inhibitor of both EGFR and ErbB2 tyrosine kinases, also demonstrated modest activity in HCC in a preliminary report.[52] Among the first 17 patients with advanced HCC, two patients had a confirmed PR and an additional eight patients had SD. However, the progression-free survival was only 2.3 months in this cohort. For another dual inhibitor, BMS-599626, a phase II clinical trial is ongoing in patients with HCC.

Cetuximab (Erbitux, IMC-C225), a chimeric monoclonal antibody against EGFR, has attracted attention in colorectal cancer as a K-Ras biomarker.[53,54] Cetuximab was also tested in two phase II studies in patients with advanced HCC. Zhu *et al.* reported five patients with SD in 30 patients with advanced HCC.[55] The median overall survival was 9.6 months, and the median progression-free survival was 1.4 months. Gruenwald *et al.* reported their preliminary experience of cetuximab in a similarly designed study in patients with HCC.[56] Of the 32 patients who were enrolled, 27 patients were evaluable for efficacy. No responses were observed, and the median time to progression for all patients was 8 weeks. The combination of cetuximab with GEMOX was evaluated in a phase II study.[57] Of the 43 patients who were enrolled, 35 patients were evaluable for efficacy, with a response rate of 23%. Given the known antitumor activity of GEMOX in prior phase II studies and the lack of activity of cetuximab as a single agent, the relative contribution of cetuximab to this regimen remains to be defined. The axis of TGF-α–EGFR signaling might be an attractive therapeutic target as frequent mutations have not been found in downstream molecules, such as Ras and Raf family members, in HCC.

Insulin-like growth factor and IGF receptor family

There is compelling evidence that both of the insulin-like growth factors IGF-I and IGF-II and their receptor IGF-1R are involved in the development and progression of cancer[58] (Fig. 1c). Interaction of IGF-I and IGF-II with IGF-1R plays a pivotal role in the tumorigenesis, proliferation, and spread of

doi: 10.1111/j.1349-7006.2008.01006.x

many cancers by promoting cell-cycle progression, preventing apoptosis, and regulating and maintaining the tumorigenic phenotype. A wide variety of tumors (including HCC) show abnormal or enhanced expression of IGF and IGF-1R, which has been correlated with disease stage, reduced survival, development of metastases, and tumor dedifferentiation.[59] We have previously identified insulin receptor substrate (IRS)-1, the main substrate of IGF-1R/insulin receptor (IR),[60,61] as an overexpressed molecule with significant roles in hepatocarcinogenesis.[62,63] Interestingly, serine phosphorylated IRS-1 protein by TNF-α is converted into an inhibitor of IGF-1R/IR.[64] Obesity and diabetes are clearly associated with an increased risk of HCC, and this seems to be due to alterations in the IGF signaling systems.

Several approaches have demonstrated the therapeutic potential of interfering with IGF-1R-mediated signaling *in vitro* and *in vivo*. Specific IGF receptor (IGFR) antibodies have also been shown to suppress prostate and breast cancer cell growth in a recent preclinical study.[65] The most advanced clinical anti-IGFR antibody is *IMC-A12*, which is currently being tested in a phase II trial for HCC. Importantly, IGFR inhibition appears to be well tolerated in the preliminary clinical studies conducted so far.[66] Safety is important, as IGFR-based inhibition has long been regarded as a high-risk intervention because of the high homology of IGF-1R with the related IR, and there is a fear that IGF-1R-tyrosine kinase inhibitors in particular might also block IR, which could lead to insulin resistance and overt diabetes.[67] However, the current *in vivo* studies did not confirm this apprehension, resulting in growing interest in anti-IGFR-based therapies. OSI-906, an IGF-1R tyrosine kinase inhibitor, is currently being tested in phase I trials for solid tumors including pancreatic cancer. The most promising IGF- and IGFR-targeted agents are currently under intense investigation in preclinical and early clinical trials.[68]

Intracellular signaling pathways

Activated RTK stimulate several intracellular signal transduction pathways, including Ras–Raf–MEK–MAPK and PI3K–Akt–mammalian target of rapamycin (mTOR) (Fig. 2).[69] In a series of specific phosphorylation events, the adaptor protein Grb2 stimulates sun of sevenless (SOS), leading to the activation of Ras, which is farnesylated and localized under the cell membrane. Farnesyl transferase inhibitors have been used in clinical trials of pancreatic cancer treatments, usually with mutations in the K-ras oncogene.[70] In spite of the low incidence of Ras gene mutations in HCC, silencing of the *RASSF1A* gene (a member of the Ras inhibitor family) with DNA methylation was found frequently in human HCC.[71] Inactivation of the Ras inhibitor might result in persistent activation of the downstream pathway during hepatocarcinogenesis. The activated form of Ras then stimulates Raf serine-threonine kinase. As mentioned above, Raf kinase is one of the targets of the multikinase inhibitor sorafenib.[1,28] Activated Raf kinase phosphorylates MEK kinases, which activate the extracellular regulated kinases Erk1/2 of the MAPK family. A MEK kinase inhibitor, AZD6244 (ARRY-142886), has been evaluated for HCC treatment in a phase II clinical trial. Once activated, Erk1/2 translocates to the nucleus where it acts as a regulator of gene expression, including those for proteins involved in cell cycle progression, apoptosis resistance, and cellular motility.[72]

The PI3K–Akt–mTOR pathway has emerged as a contributor to hepatocarcinogenesis.[73] PI3K consists of p85 adaptor and p110 kinase subunits. After association with the intracellular domain of several RTK or specific substrates such as IRS-1, PI3K phosphorylates phosphatidylinositol 3,4,5-trisphosphate (PIP3) to generate phosphatidylinositol 4,5-bisphosphate (PIP2), which transduces phosphoinositide-dependent kinase (PDK), which in turn activates the serine-threonine kinase Akt.[72] PIP3 is dephosphorylated by phospharase and tensin homologue (PTEN), a tumor suppressor, which reverses this pathway. Once activated, Akt regulates multiple cellular target proteins, including mTOR, IκB kinase (IKK), Bad, and Gsk3. The mTOR protein regulates phosphorylation of the p70 S6 serine-threonine kinase and the translational repressor protein 4E-BP1.[74] Both proteins regulate the translation of proliferative and angiogenic factors, such as c-myc, cyclin-D1, and HIF1-α, and are indirectly involved in the expression of VEGF.[75] The mTOR inhibitors temsirolimus (CCI-779) and everolimus (RAD001) have been developed as rapamycin derivates.[76,77] A phase I clinical trial using rapamycin and bevacizumab and a phase I and II clinical trial using everolimus are ongoing in patients with HCC.[76]

Another downstream protein of Akt, IKK, provokes subsequent activation of the transcription factor nuclear factor (NF)-κB.[78] NF-κB promotes cell survival by activating transcription of normally repressed target genes by binding the specific inhibitor IκB, which sequesters the NF-κB p50–p65 heterodimer in the cytoplasm.[79] Inhibition is reversed in response to several intracellular stimuli, resulting in targeted, ubiquitin–proteasome-mediated degradation of IκB.[80] The proteasome is a 26S multiprotein complex that consists of a 19S regulatory subunit and a 20S catalytic subunit. Ubiquitinated proteins are recognized by the 19S unit, which results in the liberation of ubiquitin chains that are recycled and the formation of a denatured protein that is transferred to the outer ring or the 20S core unit. Bortezomib (Velcade, PS-341) is a potent and selective inhibitor of the 20S proteasome.[81] The actions of bortezomib are pleiotropic and include inhibition of NF-κB activation by preventing IκB degradation. 26S proteasome-mediated protein degradation is a central metabolic and regulatory process in cell physiology. Apart from its role in scavenging damaged proteins, the 26S complex is an important regulator of cell life and fate. For instance, specific ubiquitination of key proteins, such as cyclins A, B, D, and E, eEF2-kinase, c-Myc, Notch, c-Jun, p21WAF/CIP1, p27, p53, topoisomerases I and II, the apoptosis modulators XIAP, Bik/NBK, Bad and Bid, the transcription coactivator β-catenin, and the NF-κB regulator IκB, targets these proteins toward proteasome degradation.[80] Through its regulation of protein turnover, the 26S proteasome is thus involved in cell-cycle progression, apoptosis, and other processes like angiogenesis and cell motility that are important in cancer progression. With the unique and independent anti-tumor effects of bortezomib, combination therapy with other cytotoxic or molecular-targeting agents is expected. Bortezomib received approval for second-line therapy of patients with progressive multiple myeloma,[80] and a phase I and II study for HCC is ongoing.[82] Because abnormalities of intracellular signal transduction pathways should play essential roles in carcinogenesis and cancer progression, further studies should be carried out.

Aurora kinases and mitotic catastrophe

Cell-cycle checkpoints are pivotal mechanisms safeguarding genomic stability. Cells that harbor defects in checkpoints are predisposed to genomic instability and neoplastic transformation. Of all the different checkpoint controls, the most important one is the mitotic spindle checkpoint, which is considered the primary defense against aneuploidy and ensures accurate chromosome segregation to produce genetically identical daughter cells (Fig. 3a).[83] Among spindle checkpoint kinases, the Aurora family of serine-threonine kinases has recently emerged as a key mitotic regulator required for genomic stability.[84] Aberrant expression of the Aurora kinase family has been reported in a variety of solid tumors. In mammals, the Aurora family consists of three members: A, B, and C. Aurora kinase A plays important roles in centrosome maturation and separation, and acentrosomal and centrosomal spindle assembly. Recent studies revealed that

Aurora kinase A also controls spindle axis orientation during asymmetric division of stem cells. Abnormalities of asymmetric division were detected in *Drosophila* that had a mutation in the mitotic kinase Aurora A, resulting in massive overproliferation in tumors.[85] Thus, the cell fate of cancer stemness might be regulated by Aurora kinase.

Aurora kinase B, another member of the family, is a chromosomal passenger protein that regulates accurate chromosomal segregation, cytokinesis, protein localization to the centromere and kinetochore, correct microtubule–kinetochore attachments, and regulation of the mitotic checkpoint.[86] Recently, we identified overexpression of Aurora kinase B as the only independent factor predictive of aggressive recurrence of HCC, based on analysis of genome-wide microarray profiling on clinical samples.[87,88] It is of interest that Aurora kinase B overexpression is closely correlated with genetic instability of HCC. Several small-molecule inhibitors of Aurora kinases have been developed as potential anticancer agents, including ZM447439,[89] hesperadin,[90] VX-680,[91] PHA-680632,[92] and MLN 8054.[93] Aurora kinase inhibitors such as AT9283 and AZD1152[94] are currently undergoing phase I clinical evaluation as treatments for malignancies.[95]

Aurora kinase B, in particular, may be a suitable anticancer target as its inhibition rapidly results in catastrophic mitosis with senescence.[95,96] During mitotic karyokinesis under downregulation of Aurora kinases, a process termed micronucleation occurs in the cancer cells. Thus, unable to maintain G_2 arrest, they enter mitosis and after being arrested for several hours at metaphase, they eventually die without successfully completing mitosis. This process is known as p53-independent cell death or mitotic catastrophe (Fig. 3b).[96] In our studies, a selective Aurora kinase B inhibitor induced *in vitro* polyploidy of human HCC cells, resulting in mitotic catastrophe. Our preclinical studies using the Aurora kinase B inhibitor revealed remarkable anti-tumor effects on HCC models *in vivo*. The inhibitor was well tolerated within the dose range required to elicit a potent and durable effect in mice. Specific inhibition of Aurora kinases is a promising novel therapeutic approach for the treatment of HCC. Further studies and clinical trials of Aurora inhibitors will confirm their significance in HCC therapeutics.

Conclusion

The concept of targeted therapies that specifically inhibit molecular abnormalities has emerged as a promising approach for the innovative and effective medical treatment of various cancers, including HCC. In this regard, sorafenib must throw new light and impact on studies of molecularly targeted agents in HCC.[6] However, although the SHARP study revealed positive and landmark results, the benefits of sorafenib were reported to be relatively modest in patients with HCC.[1] Furthermore, biomarkers to predict its effects are poorly understood. Future research should continue to unravel the mechanism of hepatocarcinogenesis and to identify key relevant molecular targets for therapeutic intervention. The advantages of molecular targeting are being explored in combination treatments as well as adjuvant or neoadjuvant therapies with surgical resection, liver transplantation, radiofrequency and transarterial chemoembolization.[4] We are only now at the beginning of the history of finding novel treatments for HCC.

References

1 Llovet JM, Ricci S, Mazzaferro V *et al.* Sorafenib in advanced hepatocellular carcinoma. *N Engl J Med* 2008; **359**: 378–90.
2 Farazi PA, DePinho RA. Hepatocellular carcinoma pathogenesis: from genes to environment. *Nat Rev Cancer* 2006; **6**: 674–87.
3 Ince N, Wands JR. The increasing incidence of hepatocellular carcinoma. *N Engl J Med* 1999; **340**: 798–9.
4 Arii S, Yamaoka Y, Futagawa S *et al.* Results of surgical and nonsurgical treatment for small-sized hepatocellular carcinomas: a retrospective and nationwide survey in Japan. The Liver Cancer Study Group of Japan. *Hepatology* 2000; **32**: 1224–9.
5 Tanaka S, Sugimachi K, Maehara S *et al.* Oncogenic signal transduction and therapeutic strategy for hepatocellular carcinoma. *Surgery* 2002; **131**: S142–7.
6 Zhu AX. Development of sorafenib and other molecularly targeted agents in hepatocellular carcinoma. *Cancer* 2008; **112**: 250–9.
7 Tanaka S, Arii S. Current status of perspective of antiangiogenic therapy for cancer: hepatocellular carcinoma. *Int J Clin Oncol* 2006; **11**: 82–9.
8 Hopfner M, Schuppan D, Scherubl H. Growth factor receptors and related signalling pathways as targets for novel treatment strategies of hepatocellular cancer. *World J Gastroenterol* 2008; **14**: 1–14.
9 Tanaka S, Sugimachi K, Yamashita Yi *et al.* Tie2 vascular endothelial receptor expression and function in hepatocellular carcinoma. *Hepatology* 2002; **35**: 861–7.
10 Shibuya M, Claesson-Welsh L. Signal transduction by VEGF receptors in regulation of angiogenesis and lymphangiogenesis. *Exp Cell Res* 2006; **312**: 549–60.
11 Tammela T, Enholm B, Alitalo K, Paavonen K. The biology of vascular endothelial growth factors. *Cardiovasc Res* 2005; **65**: 550–63.
12 Mise M, Arii S, Higashituji H *et al.* Clinical significance of vascular endothelial growth factor and basic fibroblast growth factor gene expression in liver tumor. *Hepatology* 1996; **23**: 455–64.
13 Ng IO, Poon RT, Lee JM, Fan ST, Ng M, Tso WK. Microvessel density, vascular endothelial growth factor and its receptors Flt-1 and Flk-1/KDR in hepatocellular carcinoma. *Am J Clin Pathol* 2001; **116**: 838–45.
14 Li XM, Tang ZY, Zhou G, Liu YK, Ye SL. Significance of vascular endothelial growth factor mRNA expression in invasion and metastasis of hepatocellular carcinoma. *J Exp Clin Cancer Res* 1998; **17**: 13–17.
15 El Assal ON, Yamanoi A, Soda Y *et al.* Clinical significance of microvessel density and vascular endothelial growth factor expression in hepatocellular carcinoma and surrounding liver: possible involvement of vascular endothelial growth factor in the angiogenesis of cirrhotic liver. *Hepatology* 1998; **27**: 1554–62.
16 Sugimachi K, Tanaka S, Taguchi K, Aishima S, Shimada M, Tsuneyoshi M. Angiopoietin switching regulates angiogenesis and progression of human hepatocellular carcinoma. *J Clin Pathol* 2003; **56**: 854–60.
17 Yasuda S, Arii S, Mori A *et al.* Hexokinase II and VEGF expression in liver tumors: correlation with hypoxia-inducible factor 1 alpha and its significance. *J Hepatol* 2004; **40**: 117–23.
18 von Marschall Z, Cramer T, Hocker M, Finkenzeller G, Wiedenmann B, Rosewicz S. Dual mechanism of vascular endothelial growth factor upregulation by hypoxia in human hepatocellular carcinoma. *Gut* 2001; **48**: 87–96.
19 Tsukamoto A, Kaneko Y, Yoshida T, Ichinose M, Kimura S. Regulation of angiogenesis in human hepatomas: possible involvement of p53-inducible inhibitor of vascular endothelial cell proliferation. *Cancer Lett* 1999; **141**: 79–84.
20 Lee SW, Lee YM, Bae SK, Murakami S, Yun Y, Kim KW. Human hepatitis B virus X protein is a possible mediator of hypoxia-induced angiogenesis in hepatocarcinogenesis. *Biochem Biophys Res Commun* 2000; **268**: 456–61.
21 Tanaka S, Mori M, Sakamoto Y, Makuuchi M, Sugimachi K, Wands JR. Biologic significance of angiopoietin-2 expression in human hepatocellular carcinoma. *J Clin Invest* 1999; **103**: 341–5.
22 Holash J, Maisonpierre PC, Compton D *et al.* Vessel cooption, regression, and growth in tumors mediated by angiopoietins and VEGF. *Science* 1999; **284**: 1994–8.
23 Schmitt M, Horbach A, Kubitz R, Frilling A, Haussinger D. Disruption of hepatocellular tight junctions by vascular endothelial growth factor (VEGF): a novel mechanism for tumor invasion. *J Hepatol* 2004; **41**: 274–83.
24 Arii S. Role of vascular endothelial growth factor on the invasive potential of hepatocellular carcinoma. *J Hepatol* 2004; **41**: 333–5.
25 Kaplan RN, Riba RD, Zacharoulis S *et al.* VEGFR1-positive haematopoietic bone marrow progenitors initiate the pre-metastatic niche. *Nature* 2005; **438**: 820–7.
26 Hiratsuka S, Watanabe A, Aburatani H, Maru Y. Tumour-mediated upregulation of chemoattractants and recruitment of myeloid cells predetermines lung metastasis. *Nat Cell Biol* 2006; **8**: 1369–75.
27 Gao D, Nolan DJ, Mellick AS, Bambino K, McDonnell K, Mittal V. Endothelial progenitor cells control the angiogenic switch in mouse lung metastasis. *Science* 2008; **319**: 195–8.

doi: 10.1111/j.1349-7006.2008.01006.x